Competition alters predicted forest carbon cycle responses to nitrogen availability and elevated CO_2: simulations using an explicitly competitive, game-theoretic vegetation demographic model

Ensheng Weng[1,2], Ray Dybzinski[3], Caroline E. Farrior[4], Stephen W. Pacala[5]

[1]Center for Climate Systems Research, Columbia University, New York, NY 10025

[2]NASA Goddard Institute for Space Studies, 2880 Broadway, New York, NY 10025

[3]Institute of Environmental Sustainability, Loyola University Chicago, Chicago, IL 60660

[4] Department of Integrative Biology, University of Texas at Austin, Austin, TX 78712

[5]Department of Ecology & Evolutionary Biology, Princeton University, Princeton, NJ 08544

Corresponding author: Ensheng Weng (wengensheng@gmail.com; phone: 212-678-5585)

Key words: Allocation; Biome Ecological strategy simulator (BiomeE); Competitively-optimal strategy; Game theory; Nitrogen cycle

Abstract: Competition is a major driver of carbon allocation to different plant tissues (e.g. wood, leaves, fine roots), and allocation, in turn, shapes vegetation structure. To improve their modeling of the terrestrial carbon cycle, many Earth system models now incorporate vegetation demographic models (VDMs) that explicitly simulate the processes of individual-based competition for light and soil resources. Here, in order to understand how these competition processes affect predictions of the terrestrial carbon cycle, we simulate forest responses to elevated CO_2 along a nitrogen availability gradient using a VDM that allows us to compare fixed allocation strategies versus competitively-optimal allocation strategies. Our results show that competitive and fixed strategies predict opposite fractional allocation to fine roots and wood, though they predict similar changes in total NPP along the nitrogen gradient. The competitively-optimal allocation strategy predicts decreasing fine root and increasing wood allocation with increasing nitrogen, whereas the fixed allocation strategy predicts the opposite. Although simulated plant biomass at equilibrium increases with nitrogen due to increases in photosynthesis for both allocation strategies, the increase in biomass with nitrogen is much steeper for competitively-optimal allocation due to its increased allocation to wood. The qualitatively opposite fractional allocation to fine roots and wood of the two strategies also impacts the effects of elevated [CO_2] on plant biomass. Whereas the fixed allocation strategy predicts an increase in plant biomass under elevated [CO_2] that is approximately independent of nitrogen availability, competition leads to higher plant biomass response to elevated [CO_2] with increasing nitrogen availability. Our results indicate that the VDMs that explicitly include the effects of competition for light and soil resources on allocation may generate significantly different ecosystem-level predictions of carbon storage than those that use fixed strategies.

1 Introduction

Allocation of assimilated carbon to different plant tissues is a fundamental aspect of plant growth and profoundly affects terrestrial ecosystem biogeochemical cycles (Cannell and Dewar, 1994; Lacointe, 2000). Ecologically, allocation represents an evolutionarily-honed "strategy" of plants that use limited resources and compete with other individuals and consequently drives successional dynamics and vegetation structure (De Kauwe et al., 2014; DeAngelis et al., 2012; Haverd et al., 2016; Tilman, 1988). Biogeochemically, allocation links plant physiological processes, such as photosynthesis and respiration, to biogeochemical cycles and carbon storage of ecosystems (Bloom et al., 2016; De Kauwe et al., 2014). Thus, correctly modeling allocation patterns is critical for correctly predicting terrestrial carbon cycles and Earth system dynamics.

In current Earth System Models (ESMs), the terrestrial carbon cycle is usually simulated by pool-based compartment models that simulate ecosystem biogeochemical cycles as lumped pools and fluxes of plant tissues and soil organic matter (Fig. 1: A) (Emanuel and Killough, 1984; Eriksson, 1971; Parton et al., 1987; Randerson et al., 1997; Sitch et al., 2003). In these models, the dynamics of carbon can be described by a linear system of equations (Koven et al., 2015; Luo et al., 2001; Luo and Weng, 2011; Sierra and Mueller, 2015; Xia et al., 2013):

$$\frac{dX}{dt} = AX + BU \qquad \text{(Eq. 1)}$$

where X is a vector of ecosystem carbon pools, U is carbon input (i.e., Gross Primary Production, GPP), B is the vector of allocation parameters to autotrophic respiration and plant carbon pools (e.g., leaves, stems, and fine roots), and A is a matrix of carbon transfer and turnover. In this system, carbon dynamics are defined by carbon input (U), allocation (B), and residence time and transfer coefficients (A). The allocation schemes (B) are thus embedded in a linear system, or

quasi-linear system if the allocation parameters in B are a function of carbon input (U) or plant carbon pools (X).

The modeling of allocation in this system (i.e., the parameters in vector B) is usually based on plant allometry, biomass partitioning, and resource limitation (De Kauwe et al., 2014; Montané et al., 2017). The allocation parameters are either fixed ratios to leaves, stems, and roots, which may vary among plant functional types (e.g., CENTURY, Parton et al., 1987; TEM, Raich et al., 1991; CASA, Randerson et al., 1997) or are responsive to climate and soil conditions as a way to phenomenologically mimic the shifts in allocation that are empirically observed or hypothesized (e.g., CTEM, Arora and Boer, 2005; ORCHIDEE, Krinner et al., 2005; LPJ, Sitch et al., 2003). These modeling approaches either assume that vegetation is equilibrated (fixed ratios) or average the responses of plant types to changes in environmental conditions as a collective behavior. Thus, the carbon dynamics in these models can be constrained by selecting appropriate parameters of allocation, turnover rates, and transfer coefficients to fit the observations (Friend et al., 2007; Hoffman et al., 2017; Keenan et al., 2013).

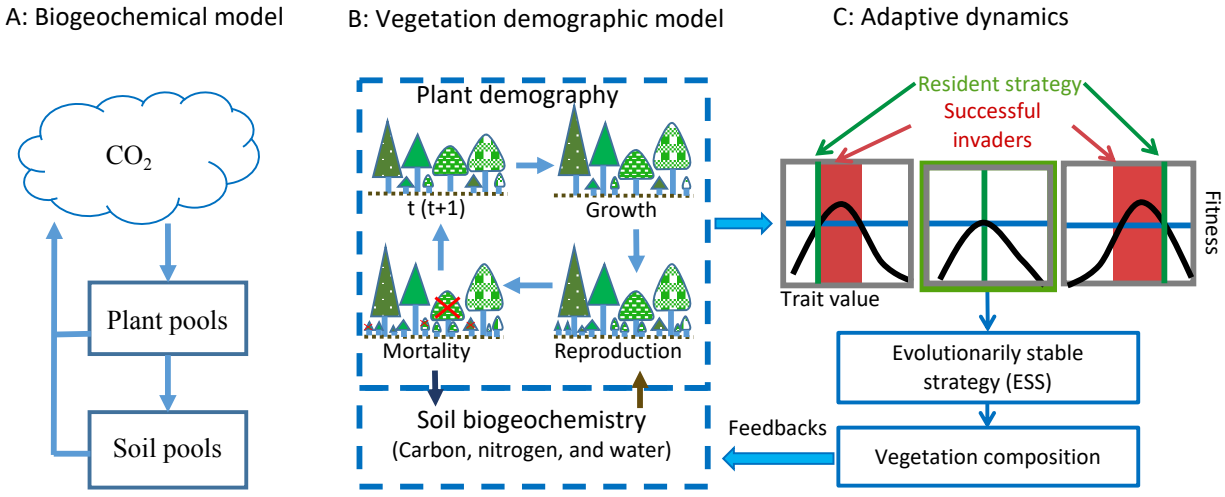

Figure 1 Hierarchical structure of vegetation models

To predict transient changes in vegetation structure and composition in response to climate change, vegetation demographic models (VDMs) that are able to simulate transient population dynamics are incorporated into ESMs (Fisher et al., 2018; Scheiter and Higgins, 2009). Generally, VDMs explicitly simulate demographic processes, such as plant reproduction, growth, and mortality, to generate the dynamics of populations (Fig. 1: B). To speed computations and minimize complexity, groups of individuals are usually modeled as cohorts. With multiple cohorts and PFTs, VDMs can bring plant functional diversity and adaptive dynamics into the system when explicitly simulating individual-based competition for different resources and vegetation succession and thus predict dominant plant traits changes with environmental conditions and ecosystem development (Scheiter et al., 2013; Scheiter and Higgins, 2009; Weng et al., 2015).

The combinations of plant traits represent the competition strategies at different stages of ecosystem development. Evolutionarily, a strategy that can outcompete all other strategies in the environment created by itself will be dominant. This strategy is called an evolutionarily stable strategy or a competitively-optimal strategy (McGill and Brown, 2007). In VDMs, competitively-optimal strategies can therefore be reasonably predicted based on the costs and benefits of different strategies (i.e., combinations of plant traits) through their effects on demographic processes (i.e., fitness) and ecosystem biogeochemical cycles (Fig. 1:C) (e.g., Farrior et al., 2015; Weng et al., 2015).

The dynamics of plant traits can substantially change predictions of ecosystem biogeochemical dynamics since they change the key parameters of vegetation physiological processes and soil organic matter decomposition (e.g., Dybzinski et al., 2015; Farrior et al., 2015; Weng et al., 2017). Therefore, the key parameters that are used to estimate carbon

dynamics in the linear system model (Eq. 1), such as allocation (B) and residence times in different carbon pools (matrix A, which includes coefficients of carbon transfer and turnover time) become functions of competition strategies that vary with environment and carbon input. In addition, the turnover of vegetation carbon pools becomes a function of allocation, leaf longevity, fine root turnover, and tree mortality rates, which change with vegetation succession and the most competitive plant traits. These changes make the system nonlinear and can lead to large biases within the framework of the compartmental pool-based models as represented by Eq. (1) (Sierra et al., 2017; Sierra and Mueller, 2015). Because of the high complexity associated with demographic and competition processes, the model predictions are usually sensitive to the parameters in these processes and are of high uncertainty (e.g., Pappas et al., 2016).

In contrast to their implementation in the more complicated VDMs discussed above, models of competitively-dominant plant strategies using much simpler model structures and assumptions can sometimes be solved analytically (Dybzinski et al., 2011, 2015; Farrior et al., 2013, 2015). Although simplified, such models can pin-point the key processes that improve the predictive power of simulation models (Dybzinski et al., 2011; Farrior et al., 2013, 2015), allowing them to help researchers formulate model processes and understand the simulated ecosystem dynamics in ESMs. For example, the analytical model derived by Farrior et al. (2013) that links interactions between ecosystem carbon storage, allocation, and water stress at elevated CO_2 sheds light on the otherwise inscrutable processes leading to varied soil water dynamics in a land model coupled with an VDM (Weng et al., 2015). Recognizing the benefit, Weng et al. (2017) included both a simplified analytical model and a more complicated VDM to understand competitively optimal leaf mass per area, competition between evergreen and deciduous plant functional types, and the resulting successional patterns.

In this study, we use a stand-alone simulator derived from the LM3-PPA model (Weng et al., 2017, 2015) to show how forests respond to elevated CO_2 and nitrogen availability via different competitively-optimal allocation strategies. The model is an individual-based vegetation demographic model, whose vegetation demographic scheme has been coupled into the land model of the Geophysical Fluid Dynamical Laboratory's Earth System Model (Shevliakova et al., 2009; Weng et al., 2015) and NASA Goddard Institute for Space Study's Earth system model, ModelE (Schmidt et al., 2014). Using this model, we simulate the shifts in competitively optimal allocation strategies in response to elevated CO_2 at different nitrogen levels based on insights from the analytical model derived by Dybzinski et al. (2015). Dybzinski et al.'s (2015) model predicts that increases in carbon storage at elevated CO_2 relative to storage at ambient CO_2 are largely independent of total nitrogen because of an increasing shift in carbon allocation from long-lived, low-nitrogen wood to short-lived, high-nitrogen fine roots under elevated CO_2 with increasing nitrogen availability. Here, we analyze the simulated ecosystem carbon cycle variables (gross and net primary production, allocation, and biomass) of separate mono- and polyculture model runs. In the monoculture runs, ecosystem properties are the result of the prescribed allocation strategies of a given PFT. In the polyculture runs, competition between the different allocation strategies results in succession and the eventual dominance of the most competitive allocation strategy for a given nitrogen availability and CO_2 level. Since everything else in the model is identical, we are able to compare the predictions of single **fixed strategies** with **competitively-optimal allocation strategies** by comparing the ecosystem properties of these two types of runs.

2 Methods and Materials

2.1 BiomeE model overview

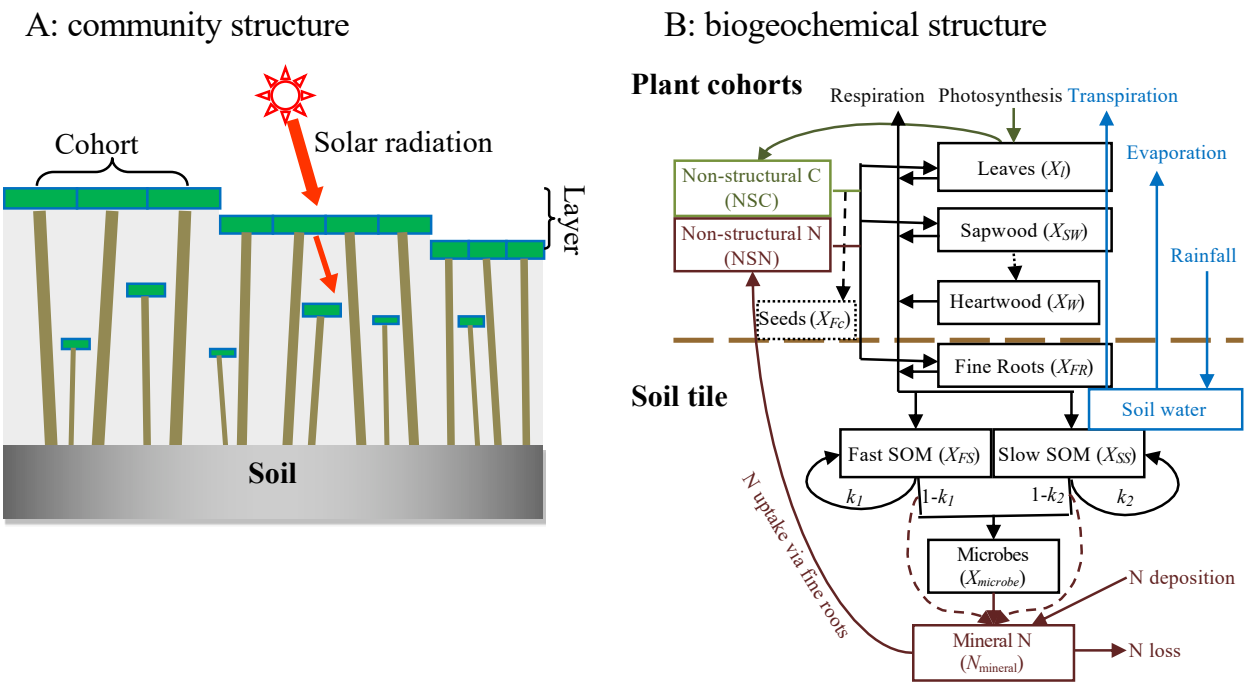

Figure 2. Structure of BiomeE

Panel A: vegetation structure: trees organize their crowns into canopy layers according to both their height and their crown area following the rules of the PPA model, which mechanistically models light competition. Panel B: Biogeochemical structure and compartmental pools. The green, brown, and black lines are the flows of carbon, nitrogen, and coupled carbon and nitrogen, respectively. The green box is for carbon only. The brown boxes are nitrogen pools. The black boxes are for both carbon and nitrogen pools, where *X* can be C (carbon) and N (nitrogen). The C:N ratios of leaves, fine roots, seeds, and microbes are fixed. The C:N ratios of woody tissues, fast soil organic matter (SOM), and slow SOM are flexible. Only one tree's C and N pools are shown in this figure. The blue box and arrows are for water storage in soil and fluxes of rainfall, evaporation, and transpiration. The model can have multiple cohorts of trees, which share the same pool structure. The dashed line separates the aboveground and belowground processes.

We used a stand-alone ecosystem simulator (Biome Ecological strategy simulator, BiomeE) to conduct simulation experiments. BiomeE is derived from the version of LM3-PPA used in Weng *et al*. (2017), and its code is available at Github (https://github.com/wengensheng/BiomeESS). In this version, we simplified the processes of energy transfer and soil water dynamics of LM3-PPA (Weng et al., 2015) but still retained the key features of plant physiology and individual-based competition for light, soil water, and, via the decomposition of soil organic matter, nitrogen (Fig. 2 and Supplementary Information I for details). In this model, individual trees are represented as sets of *cohorts* of similar size trees and are arranged in different vertical canopy layers according to their height and crown area following the rules of the Perfect Plasticity Approximation (PPA) model (Strigul et al., 2008). Sunlight is partitioned into these canopy layers according to Beer's law. Thus, a key parameter for light competition, critical height, is defined; all the trees above this context-dependent height get full sunlight and all trees below this height are shaded by the upper layer trees.

Each tree consists of seven pools: leaves, fine roots, sapwood, heartwood, fecundity (seeds), and non-structural carbohydrates and nitrogen (NSC and NSN, respectively) (Fig. 2: b). The carbon and nitrogen in plant pools enter the soil pools with the mortality of individual trees and the turnover of leaves and fine roots. There are three soil organic matter (SOM) pools for carbon and nitrogen: fast-turnover, slow-turnover, and microbial pools, along with a mineral nitrogen pool for mineralized nitrogen in soil. The simulation of SOM decomposition and nitrogen mineralization is based on the models of Gerber *et al*. (2010) and Manzoni *et al*. (2010) and described in detail in Weng et al. (2017). The decomposition rate of a SOM pool is determined by the basal turnover rate together with soil temperature and moisture. The nitrogen mineralization rate is a function of decomposition rate and the C:N ratio of the SOM. Microbes

must consume more carbon in the high C:N ratio SOM pool to get enough nitrogen and must release excessive nitrogen in the low C:N ratio SOM pool to get enough carbon for energy (Weng *et al*. 2017).

Table 1 Model parameters

Symbol	Definition	Unit	Default value	Reference
α_Z	Parameter of tree height	m $m^{-0.5}$	36	Farrior et al., 2013
θ_Z	Diameter exponent of tree height	-	0.5	Farrior et al., 2013
Λ	Taper factor	-	0.75	Weng et al. 2015
ρ_W	Wood density	kgC m^{-3}	300	(Jenkins et al., 2003)
α_C	Parameter of crown area	m $m^{-1.5}$	150	Farrior et al., 2013
θ_C	Diameter exponent of crown area	-	1.5	Farrior et al., 2013
l^*	Target crown leaf area layers (crown leaf area index)	m^2 m^{-2}	3.5	-
σ	Leaf mass per unit area	kgC m^{-2}	0.14	(Wright et al., 2004)
γ	Specific root area, calculated from root radius and density	m^2 kgC^{-1}	34.5	(Pregitzer et al., 2002)
φ_{RL}	Ratio of target fine root area to target leaf area	m^2 m^{-2}	Varied with PFTs	-
α_{CSA}	ratio of target sapwood cross-sectional area to target leaf area	m^2 m^{-2}	$0.2x10^{-4}$	(McDowell et al., 2002)
$f_{U,max}$	Maximum mineral nitrogen absorption rate	$hour^{-1}$	0.5	-
K_{FR}	Root biomass at which the N-uptake rate is half of the maximum	kgC m^{-2}	0.3	-
$CN_{L,0}$	Target C:N ratio of leaves	kgC kgN^{-1}	76.5 (Function of LMA)	(Wright et al., 2004)
$CN_{FR,0}$	Target C:N ratio of fine roots	kgC kgN^{-1}	60	(Magill et al., 2004)
$CN_{W,0}$	Target C:N ratio of wood	kgC kgN^{-1}	350	(Martin et al., 2015)
$CN_{F,0}$	Target C:N ratio of seeds	kgC kgN^{-1}	20	(Soriano et al., 2011)
f_1	Supply rate of NSC and NSN	-	1/(3*365)	-
f_2	Maximum fraction of NSC and NSN used for growth in a day	-	0.02	-

$f_{LFR,max}$	Maximum fraction of available carbon allocated to leaves and fine roots	-	0.85	-
v	Fraction of carbon converted to seeds	-	0.1	-
$r_{D/S}$	Nitrogen-limiting factor	-	Solved by the model (Eqs 9 and 10)	-

Plant growth and reproduction are driven by the carbon assimilation of leaves via photosynthesis, which is in turn dependent on water and nitrogen uptake by fine roots. The photosynthesis model is identical to that of LM3-PPA (Weng et al., 2015), which is a simplified version of Leuning model (Leuning et al., 1995). This model first calculates photosynthesis rate, stomatal conductance, and water demand of the leaves of each tree (cohort) in the absence of soil water limitation. Then, it calculates available water supply as a function of fine root surface area and soil water content. The demand-based assimilation rate and stomatal conductance are adjusted if soil water supply is less than plant water demand. Soil water content is calculated based on the fluxes of precipitation, soil surface evaporation, and plant water update (transpiration) in three layers of soil to a depth of 2 meters. (Please see Supplementary Information I for details).

Assimilated carbon enters into the NSC pool and is subsequently used for respiration, growth, and reproduction. Empirical allometric equations relate woody biomass (including coarse roots, bole, and branches), crown area, and stem diameter. The individual-level dimensions of a tree, *i.e.*, height (Z), biomass (S), and crown area (A_{CR}) are given by empirical allometries (Dybzinski et al., 2011; Farrior et al., 2013):

$$\begin{aligned} Z(D) &= \alpha_Z D^{\theta_Z} \\ S(D) &= 0.25\pi\Lambda\rho_W\alpha_Z D^{2+\theta_Z} \\ A_{CR}(D) &= \alpha_c D^{\theta_c} \end{aligned} \qquad \text{(Eq. 2)}$$

where Z is tree height, D is tree diameter, S is total woody biomass carbon (including bole, coarse roots, and branches) of a tree, α_c and α_Z are PFT-specific constants, θc=1.5 and θ_Z=0.5 (Farrior et al., 2013) (although they could be made PFT-specific if necessary), π is the circular constant, Λ is a PFT-specific taper constant, and ρ_W is PFT-specific wood density (kg C m^{-3}) (Table 1).

We set *targets* for leaf (L^*), fine root (FR^*), and sapwood cross-sectional area (A^*_{SW}) that govern plant allocation of non-structural carbon and nitrogen during growth. These *targets* are related by the following equations based on the assumption of the pipe model (Shinozaki, Kichiro et al., 1964):

$$\begin{aligned} L^*(D,p) &= l^* \cdot A_{CR}(D) \cdot \sigma \cdot p(t) \\ FR^*(D) &= \varphi_{RL} \cdot l^* \cdot \frac{A_{CR}(D)}{\gamma} \\ A^*_{SW}(D) &= \alpha_{CSA} \cdot l^* \cdot A_{CR}(D) \end{aligned} \qquad \text{(Eq. 3)}$$

where L^* (D, p), $FR^*(D)$, and $A^*_{SW}(D)$ are the targets of leaf mass (kg C/tree), fine root biomass (kg C/tree), and sapwood cross sectional area (m^2/tree), respectively, at tree diameter D; l^* is the target leaf area per unit crown area of a given PFT; A_{CR}(D) is the crown area of a tree with diameter D; σ is PFT-specific leaf mass per unit area (LMA); and $p(t)$ is a PFT-specific function ranging from zero to one that governs leaf phenology (Weng et al., 2015); φ_{RL} is the target ratio of total root surface area to the total leaf area; γ is specific root area; and α_{CSA} is an empirical constant (the ratio of sapwood cross-sectional area to target leaf area). The phenology function p(t) takes values 0 (non-growing season) or 1 (growing season) following the phenology model of LM3-PPA (Weng et al., 2015). The onset of a growing season is controlled by two variables, growing degree days (GDD), and a weighted mean daily temperature (T_{pheno}), while the end of a

growing season is controlled by T_{pheno}. (Please see Supplementary Information I for details of the phenology model)

Nitrogen uptake

The rate of nitrogen uptake (U, g N m^{-2} hour^{-1}) from the soil mineral nitrogen pool is an asymptotically increasing function of fine root biomass density ($C_{FR,total}$, kg C m^{-2}), following McMurtrie *et al*. (2012)

$$U = f_{U,max} \cdot N_{mineral} \cdot \frac{C_{FR,total}}{C_{FR,total}+K_{FR}}, \quad \text{(Eq. 4)}$$

where, $N_{mineral}$ is the mineral nitrogen in soil (g N m^{-2}), $f_{U,max}$ is the maximum rate of nitrogen absorption per hour when $C_{FR,total}$ approaches infinity, K_{FR} is a shape parameter (kg C m^{-2}) at which the nitrogen uptake rate is half of the parameter f_U,max. The nitrogen uptake rate of an individual tree (U_{tree}, kg N hour^{-1} tree^{-1}) is calculated as follows:

$$U_{tree} = U \cdot \frac{C_{FR,tree}}{C_{FR,total}}, \quad \text{(Eq. 5)}$$

where, $C_{FR,tree}$ is the fine root biomass of a tree (kgC tree^{-1}). The nitrogen absorbed by roots enters into the NSN pool and then is allocated to plant tissues through plant growth.

Allocation and plant growth

The partitioning of carbon and nitrogen into the plant pools (*i.e.*, leaves, fine roots, and sapwood) is limited by the allometric equations, targets of leaves, fine roots, and sapwood cross-sectional area, and the stoichiometry (i.e., C:N ratios) of these plant tissues. At a daily time step, the model calculates the amount of carbon and nitrogen that are available for growth according to the total NSC and NSN and current leaf and fine root biomass. Basically, the available NSC (G_C) is the summation of a small fraction (f_l) of the total NSC in an individual plant and the

differences between the targets of leaf and fine roots and their current biomass capped by a larger fraction (f_2) of NSC (Eq. 6.1). The available NSN (G_N) is analogous to that of the NSC and meets approximately the stoichiometrical requirement of plant tissues (Eq. 6.2).

$$G_C = \min\left(f_1 NSC + L^* + FR^* - L - FR, f_2 NSC\right) \quad \text{(Eq. 6.1)}$$

$$G_N = \min\left(f_1 NSN + N_L^* + N_{FR}^* - N_L - N_{FR}, f_2 NSN,\right) \quad \text{(Eq. 6.2)}$$

where L^* and FR^* are the targets of leaves and fine roots, respectively (see Eq. 3); L and FR are current leaf and fine roots biomass, respectively; N_L^* and N_{FR}^* are nitrogen of leaves and fine roots at their targets according to their target C:N ratios. The parameter f_2 gives the daily availability of NSC during periods of leaf flush at the beginning of a growing season and f_1 normal growth of stems after plant leaves and fine roots approach their targets. Usually, parameter f_1 is much greater than f_2. We let f_1=0.02 and f_2= 1/(365x3) in this study.

The allocation of the available NSC (i.e., G_C) to wood (G_W), leaves (G_L), fine roots (G_{FR}), and seeds (G_F) follows the equations below (Eq. 7). These equations describe the mass growth of plant tissues with nitrogen effects on the carbon allocation between high-nitrogen tissues and low-nitrogen tissues (wood) for maximizing leaves and fine roots growth (G_L and G_{FR}, respectively), optimizing carbon usage at given nitrogen supply (G_N), and keeping the tissues at their target C:N ratios.

$$G_C \geq G_W + G_L + G_{FR} + G_F \quad \text{(Eq. 7.1)}$$

$$G_N \geq \frac{G_L}{CN_{L,0}} + \frac{G_{FR}}{CN_{FR,0}} + \frac{G_F}{CN_{F,0}} + \frac{G_W}{CN_{W,0}} \quad \text{(Eq. 7.2)}$$

$$\frac{(FR+G_{FR})\gamma}{(L+G_L)/\sigma} = \varphi_{RL} \quad \text{(Eq. 7.3)}$$

$$G_L + G_{FR} = Min\begin{pmatrix} L^* + FR^* - L - FR, \\ f_{LFR,max}\, G_C \end{pmatrix} \cdot r_{S/D} \quad \text{(Eq. 7.4)}$$

$$G_F = \left[G_C - Min\begin{pmatrix} L^* + FR^* - L - FR, \\ f_{LFR,max}\, G_C \end{pmatrix} r_{S/D}\right] \cdot v \cdot r_{S/D} \quad \text{(Eq. 7.5)}$$

$$G_W = \left[G_C - Min\begin{pmatrix} L^* + FR^* - L - FR, \\ f_{LFR,max}\, G_C \end{pmatrix} r_{S/D}\right] \cdot (1 - v \cdot r_{S/D}) \quad \text{(Eq. 7.6)}$$

where, $CN_{L,0}$, $CN_{FR,0}$, $CN_{F,0}$, and $CN_{W,0}$ are the target C:N ratios of leaves, fine roots, seeds, and sapwood, respectively; γ is specific root area (m^2 kgC^{-1}); σ is leaf mass per unit area (kg C m^{-2}); $f_{LFR,max}$ is the maximum fraction of G_C for leaves and fine roots (0.85 in this study); v is the fraction of left carbon for seeds (0.1 in this study); $r_{S/D}$ is a nitrogen-limiting factor ranging from 0 (no nitrogen for leaves, fine roots, and seeds) to 1 (nitrogen available for full growth of leaves, fine roots, and seeds). The parameter $r_{S/D}$ controls the allocation of G_C and G_N to the four plant pools (Eq. 7.1). It can be analytically solved (Eqs. 8 and 9).

$$r_{S/D} = Min\left[1, Max\left(0, \frac{G_N - G_C/CN_W}{N' - G_C/CN_W}\right)\right], \quad \text{(Eq. 8)}$$

where, N' is defined as the potential nitrogen demand for plant growth at $r_{S/D}$=1 (i.e., no nitrogen limitation).

$$N' \equiv \frac{\gamma\sigma\left[FR + Min\begin{pmatrix} L^*+FR^*-L-FR, \\ f_{LFR,max}\, G_C \end{pmatrix}\right] - \varphi_{RL} L}{(\gamma\sigma + \varphi_{RL}) CN_L} + \frac{\varphi_{RL}\left[L + Min\begin{pmatrix} L^*+FR^*-L-FR, \\ f_{LFR,max}\, G_C \end{pmatrix}\right] - \gamma\sigma L}{(\gamma\sigma + \varphi_{RL}) CN_{FR}} + \frac{v\left[G_C - Min\begin{pmatrix} L^*+FR^*-L-FR, \\ f_{LFR,max}\, G_C \end{pmatrix}\right]}{CN_F} + \frac{(1-v)\left[G_C - Min\begin{pmatrix} L^*+FR^*-L-FR, \\ f_{LFR,max}\, G_C \end{pmatrix}\right]}{CN_W}. \quad \text{(Eq. 9)}$$

When $G_N \geq N'$ ($r_{S/D}$ = 1), there is no nitrogen limitation, and all the G_C will be used for plant growth and the allocation follows the rules of the carbon only model (Eqs 7.4~7.6 as $r_{S/D}$ = 1). The excessive nitrogen (G_N–N') will be returned to the NSN pool (as if they were never taken

out). When $G_C/CN_{W,0}<G_N< N'$ (i.e., $0< r_{S/D} < 1$), all G_C and G_N will be used in new tissue growth; however, the leaves and fine roots cannot reach their targets at this step (i.e. they are down-regulated). When $G_N \leq G_C/CN_{W,0}$ ($r_{S/D} = 0$), all the G_N will be allocated to sapwood and the excessive carbon ($G_C - G_N CN_{W,0)}$ will be returned to NSC pool. This is a very rare case since a low G_N leads to low leaf growth, reducing G_C before the case $G_N<G_C/CN_{W,0}$ happens. Therefore, in most cases, Eq. 7.1 is: $G_C = G_W + G_L + G_{FR} + G_F$. Overall, this strategy down-regulates leaf production under low nitrogen conditions while making use of assimilated carbon in height-structured competition for light.

Allocation to wood tissues (G_W) drives the growth of tree diameter, height, and crown area and thus increases the targets of leaves and fine roots (Eq. 3). By differentiating the stem biomass allometry in Eq. 2 with respect to time, using the fact that dS/dt equals the carbon allocated for wood growth (G_W), we have the diameter growth:

$$\frac{dD}{dt} = \frac{G_W}{0.25\pi\Lambda\rho_W\alpha_z(2+\theta_z)D^{1+\theta_Z}} \quad \text{(Eq. 10)}$$

This equation transforms the mass growth to structural changes in tree architecture. With an updated tree diameter, we can calculate the new tree height and crown area using allometry equations (Eq. 2) and targets of leaf and fine root biomass (Eq. 3) for the next growth step.

Overall, this is a flexible allocation scheme and still follows the major assumptions in the previous version of LM3-PPA (Weng, et al., 2015, 2017). This allocation scheme prioritizes the allocation to leaves and fine roots, maintains a minimum growth rate of stems, and keeps the constant area ratio of fine roots to leaves. Based on these allocation rules, the average allocation of carbon and nitrogen to leaves, fine roots, and wood over a growing season are governed by the targets for the leaf area per unit crown area (i.e., crown leaf area index, l^*) and fine root area per

unit leaf area (φ_{RL}). Since the crown leaf area index, l^*, is fixed in this study, φ_{RL} is the key parameter determining the relative allocation of carbon to fine roots and stems. A high φ_{RL} means a high relative allocation to fine roots and therefore low relative allocation to stems, and *vice versa*. Note, here φ_{RL} is fixed for each PFT and will remain so for all the model runs.

The process of choosing a context-dependent competitively dominant φ_{RL} will take place after finding the fitness of each φ_{RL} in monoculture and in competition with other PFTs (*i.e.*, different values of φ_{RL}). The competitively optimal strategy is the one that can successfully exclude all others in the processes of competition and succession, but it is not necessarily the one that maximizes production in monoculture. For example, each φ_{RL} creates an environment of light profile and soil nitrogen in its monoculture. Other φ_{RL} PFTs may have higher fitness in this environment than the one that creates it. Only the competitively dominant strategy has the highest fitness in the environment it creates (Fig. 1: C).

2.2 Site and Data

Data pertaining to vegetation, climate, and soil at Harvard Forest (Aber et al., 1993; Hibbs, 1983; Urbanski et al., 2007) were used to design the plant functional types (PFTs) and ecosystem nitrogen levels used in the simulation experiments, to drive the model, and to calibrate model parameters. Harvard Forest is located in Massachusetts, USA (42.54°, -72.17°). The climate of Harvard Forest is cool temperate with annual precipitation 1050 mm, distributed fairly evenly throughout the year. The annual mean temperature is 8.5 °C with a high monthly mean temperature of 20°C in July and a low of -7°C in January. The soils are mainly sandy loam with average depth around 1 m and are moderately well drained in most areas. In forest sites, soil carbon is around 8 kg C m^{-2} and nitrogen 300 g N m^{-2} (Compton and Boone, 2000). The vegetation is deciduous broadleaf/mixed forest with major species red oak (*Quercus rubra*), red

maple (*Acer rubrum*), black birch (*Betula lenta*), white pine (*Pinus strobus*), and hemlock (*Tsuga canadensis*) (Compton and Boone, 2000; Savage et al., 2013). The data used to drive our model runs are gap-filled hourly meteorological data at Harvard Forest from 1991 to 2006, obtained from North American Carbon Program (NACP) Site-Level Synthesis datasets (Barr et al., 2013).

2.3 Simulation experiments

We set two atmospheric CO_2 concentration ($[CO_2]$) levels: 380 ppm and 580 ppm, and eight ecosystem total nitrogen levels (ranging from 114.5 g N m^{-2} to 552 g N m^{-2} at the interval of 62.5 g N m^{-2}) by assigning the initial content of the slow SOM pool for our simulation experiments (Table 2). This range covers the soil nitrogen contents across the plots at Harvard Forest with different species compositions and land use history (200~300 gN m^{-2}) (Compton and Boone, 2000; Melillo et al., 2011), and represents the range from infertile to fertile soils in temperate forests (Post et al., 1985; Yang et al., 2011). The nitrogen cycles through the plant and soil pools and is redistributed among them via plant demographic processes, soil carbon transfers, and plant uptake. In all the simulation experiments, we assume the ecosystem has no nitrogen inputs and no outputs for convenience since we already have eight total nitrogen levels to represent the consequences of different nitrogen input and output processes at an equilibrium state. The PFTs were based on an evergreen needle-leaved tree PFT with different leaf to fine root area ratios, φ_{RL}, in the range from 1 to 8 (Table 2). Simply stated, the PFTs we investigate only differ in parameter φ_{RL}.

We define the model runs started with only one fixed-φ_{RL} PFT as "monoculture runs" although the actual allocation of carbon to different plant tissues varies with $[CO_2]$ concentration and ecosystem nitrogen availability. The model runs started with multiple PFTs are called

339 "polyculture runs" (eight PFTs with different φ_{RL} at the beginning, although many are driven to
340 extinction during a given model run). We conducted one set of monoculture runs and two sets of
341 polyculture runs (Table 2).
342
343 **Table 2 Simulation experiments**

Type	Model runs	Initial PFT(s) φ_{RL}	Ecosystem total nitrogen levels	CO_2 concentration [CO_2]
Monoculture runs	One model run per combination of PFT (φ_{RL}), nitrogen level, and CO_2 concentration	One of the following PFTs: φ_{RL}= 1, 2, 3, 4, 5, 6, 7, or 8	Eight levels ranging from 114.5 g N m^{-2} to 552 g N m^{-2} at the interval of 62.5 g N m^{-2}: 114.5 g N m^{-2}, 177 g N m^{-2}, 239.5 g N m^{-2}, 302 g N m^{-2}, 364.5 g N m^{-2}, 427 g N m^{-2}, 489.5 g N m^{-2}, 552 g N m^{-2}	Ambient: 380 ppm Elevated: 580 ppm
Polyculture runs I	One model run per combination of nitrogen level and CO_2 concentration	All the PFTs (φ_{RL}= 1~ 8) used in the monoculture runs		
Polyculture runs II	One model run per combination of nitrogen level and CO_2 concentration	Eight PFTs with φ_{RL} ranging from 4.5-0.5*i* to 8.5-0.5*i* at the interval of 0.5, where *i* denotes the eight nitrogen levels from 114.5 to 552 gN m^{-2}.		

344
345 In the monoculture runs, we run the full combinations of eight PFTs with root/leaf area
346 ratios (φ_{RL}) from 1 to 8, eight ecosystem total nitrogen levels, and two CO_2 concentrations [CO_2]
347 (380 ppm and 580 ppm) (Table 2). For the eight PFTs, only those with φ_{RL} <=6 survived at
348 ambient [CO_2] (380 ppm) because the carbon consumed by fine roots exceeded what leaves
349 provided at φ_{RL}>6. The monoculture runs are for exploring the model predictions of gross
350 primary production (GPP), net primary production (NPP), allocation, and biomass at equilibrium

with fixed φ_{RL} and ecosystem total nitrogen levels, analogous to the functional relationship schemes used in many ecosystem models (e.g., De Kauwe et al., 2014).

In polyculture runs I, we used the same PFTs as in the monoculture runs, where their φ_{RL} varies from 1 to 8 at the interval of 1.0 and the ecosystem total nitrogen levels are the same as those used in the monoculture runs (Table 2). This set of polyculture runs was used to explore successional patterns at both ambient and elevated [CO_2] concentrations (380 ppm and 580 ppm, respectively). However, this set of model runs could not show the details of equilibrium plant biomass and allocation patterns along the nitrogen gradient because of the large intervals between the φ_{RL} values.

To achieve greater resolution in our competition predictions, we designed the polyculture runs II using a dynamic PFT combination scheme according to the ranges of φ_{RL} obtained from the polyculture runs I that could survive at a particular nitrogen level at both CO_2 concentrations. For each nitrogen level, we set eight PFTs with φ_{RL} that varied in a range 3.5 (e.g., $x \sim x$+3.5) at the interval of 0.5, starting with the highest φ_{RL} of 8.0 at the lowest N level (114.5 g N m^{-2}) and decreasing 0.5 per level of increase in ecosystem total N. We use i=1, 2, …, 8 to denote the eight N levels from 114.5 to 552 g N m^{-2}. The φ_{RL} of the eight PFTs at each level are 5.0-0.5i, 5.5-0.5i, …, 8.5-0.5i (Table 2). For example, at the nitrogen of 114.5 g N m^{-2} (i = 1), the φ_{RL} of the eight PFTs are 4.5, 5.0, …, 8.0 and at 177 g N m^{-2} (i = 2), they are 4.0, 4.5, …, 7.5.

For both monoculture and polyculture runs, visual inspection indicated that stands had reached equilibrium after ~1200 years. To be conservative, we present equilibrium data by averaging model properties between years 1400 and 1800. We compared simulated equilibrium gross primary production (GPP), net primary production (NPP), allocation (both absolute amount of carbon and fractions of the total NPP), and plant biomass of the polyculture runs II with those

374 from the monoculture runs. We used the results from one PFT (φ_{RL}=4) to highlight the
375 differences of plant responses with competitively optimal allocation strategies obtained from the
376 polyculture runs II.
377
378 **3 Results**
379 In the monoculture runs, GPP and NPP increase by a factor of three along the gradient of
380 nitrogen used in this study (114.5 - 552 g N m^{-2}) at both ambient (Fig. 3) and elevated [CO_2]
381 (Figs. S1). The magnitude of differences in GPP and NPP due to differences in fixed allocation
382 within a given nitrogen level is comparable to the magnitude of differences in GPP and NPP due
383 to nitrogen level within a given fixed allocation strategy (Fig. 3: a and b) when φ_{RL} is in the
384 range that allows plants to grow normally (1~5 in the case of ambient [CO_2]). As prescribed by
385 the definition of φ_{RL}, allocation of NPP to fine roots increases with φ_{RL} in monoculture runs (Fig.
386 3: c). As a consequence, allocation of NPP to wood decreases as φ_{RL} increases (Fig. c: d).
387 Allocation to leaves does not change much with φ_{RL}. (Fig. 3: e, note differences in scale).
388 Correspondingly, plant biomass at equilibrium decreases with φ_{RL} (Fig. 3: f). The effects of
389 nitrogen on the allocation of carbon to fine roots and wood follow our allocation model
390 assumptions because *proportionally* more carbon is allocated to low-nitrogen woody tissues in
391 our model when nitrogen is limited. However, the amplitude of changes in GPP and NPP
392 induced by nitrogen availability is lower than the amplitude of changes resulting from different
393 values of φ_{RL} in the monoculture runs.

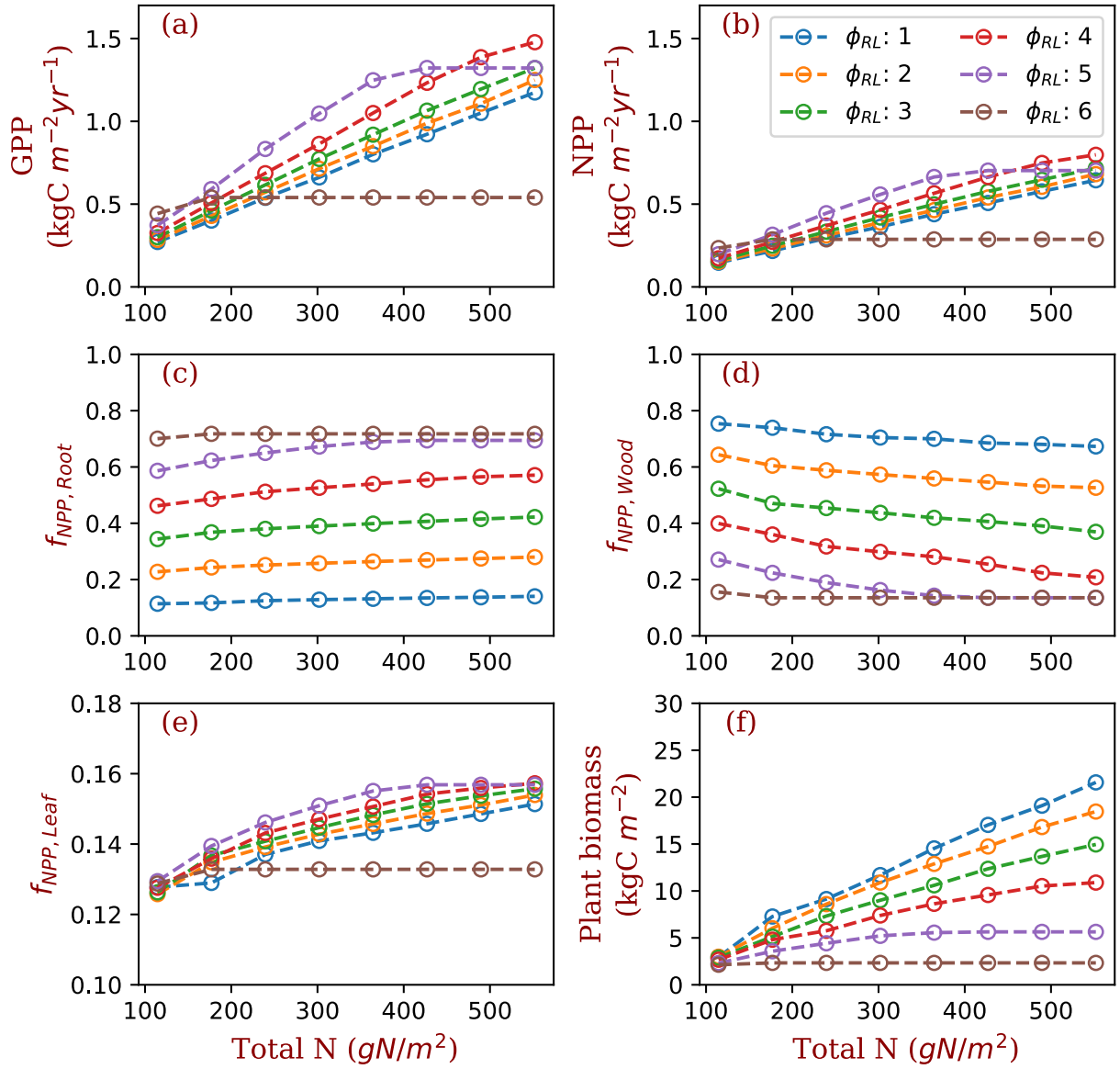

394

395 **Figure 3. GPP, NPP, Allocation and Plant biomass at equilibrium state simulated by**

396 **monoculture runs**. GPP: Gross primary production; NPP: Net primary production; $f_{\mathrm{NPP},x}$: the

397 fraction of NPP allocated to x, where x is Root (fine roots), Leaf (leaves in crown), or Wood

398 (including tree trunk, stems, and coarse roots). The data are from the averages of the model run

399 years from 1400 and 1800. Each model run is initiated with one PFT with fixed ratio of fine root

400 area to leaf area (φ_{RL}).

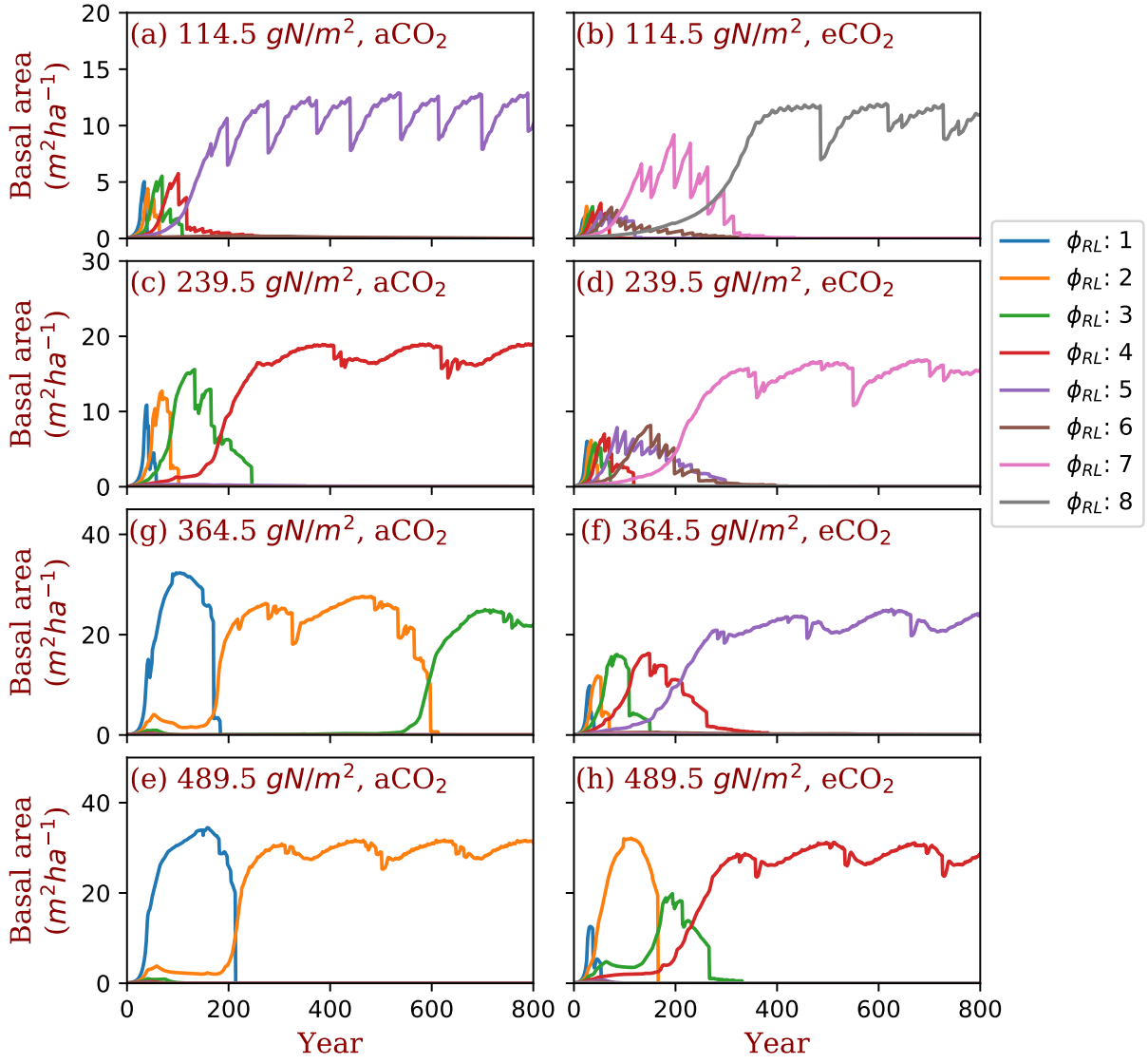

Figure 4 Successional patterns of polyculture runs I at ambient and elevated CO2 concentrations. φ_{RL} is the fixed ratio of fine root area to leaf area of a particular strategy.

We used two sets of polyculture runs to look for the φ_{RL} that is closest to competitively optimal (i.e., the evolutionarily stable strategy). In the polyculture runs I, where φ_{RL} ranges from 1 to 8 at all nitrogen levels, the winning strategy (φ_{RL}) increases from 5 to 2 as the total nitrogen increases from 114.5 g N m^{-2} to 489.5 g N m^{-2} at ambient [CO_2] (380 ppm) (Fig. 4: a, c, g, e).

Elevated [CO_2] (580 ppm) shifts the winning strategy to higher (φ_{RL}) at all the total nitrogen levels. As shown in Fig. 4, the winning strategy shifts from φ_{RL}=5 to φ_{RL}=8 at 114.5 g N m^{-2} and from φ_{RL} =2 to φ_{RL}=4 at 489.5 g N m^{-2}. In some situations (e.g., Fig. 4g and Figs. S2 and S3), it takes a long time for the most competitive PFTs to out-compete the previously dominant PFTs because of the sequential replacement of dominant PFTs during the course of succession and the slow growth rate of trees in understory.

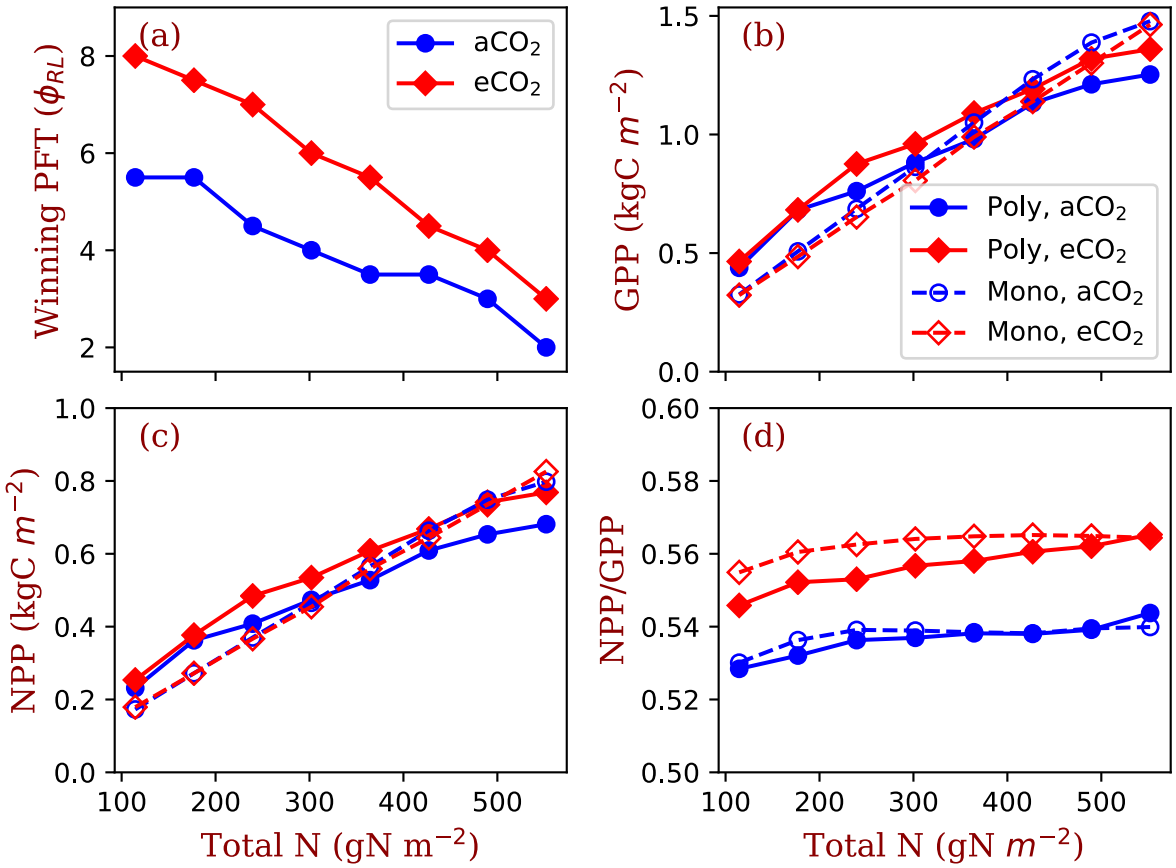

Figure 5 Winning PFTs (φ_{RL}, a) in polyculture runs II and equilibrium Gross Primary Production (GPP, b), Net Primary Production (NPP, c), and Carbon Use Efficiency (NPP/GPP, d) at two CO_2 concentrations (aCO_2: 380 ppm; eCO_2: 580 ppm). The closed symbols with solid line represent polyculture runs. The open symbols with dashed lines represent

monoculture runs (only φ_{RL}=4 shown in this figure). φ_{RL} is the fixed ratio of fine root area to leaf area of a particular strategy.

Based on the shifts of the winning φ_{RL} from ambient [CO_2] to elevated [CO_2] at the eight nitrogen levels, we designed the polyculture runs II with high resolution of φ_{RL} and calculated their GPP, NPP, allocation, and plant biomass at equilibrium state. The of φ_{RL} of the winning PFTs decreases from 5.5 to 2 at ambient [CO_2] and from 8.0 to 3.0 at elevated [CO_2] as total nitrogen increases from 114.5 gN m^{-2} to 552.0 gN m^{-2}. The equilibrium GPP and NPP increase with total nitrogen at values similar to those of the monoculture runs (Fig. 5: b and c). However, the CO_2 stimulation of NPP increases with total nitrogen in the polyculture runs more than it in the monoculture runs. Elevated [CO_2] increases carbon use efficiency (defined as the ratio of NPP to GPP in this study, NPP/GPP) in both the monoculture and polyculture runs (Fig. 5: d). Also, the dependence of NPP:GPP ratio on nitrogen is higher in the polyculture runs than it in the monoculture runs (Fig. 5:c).

Allocation of NPP to leaves increases with total nitrogen in all conditions, i.e. both competition and monoculture at both ambient [CO_2] and elevated [CO_2] (Fig. 6: a). Foliage NPP is similar in these four model runs when nitrogen is low. At high nitrogen (>400 g N m^{-2}), polyculture runs have higher foliage NPP than the monoculture runs generally. Allocation to leaves is relatively stable across the nitrogen gradient at the two [CO_2] levels (Fig. 6: b). The fraction of NPP allocated to leaves changes little with nitrogen (Fig. 6: b) and it is universally higher at ambient [CO_2] than at elevated [CO_2].

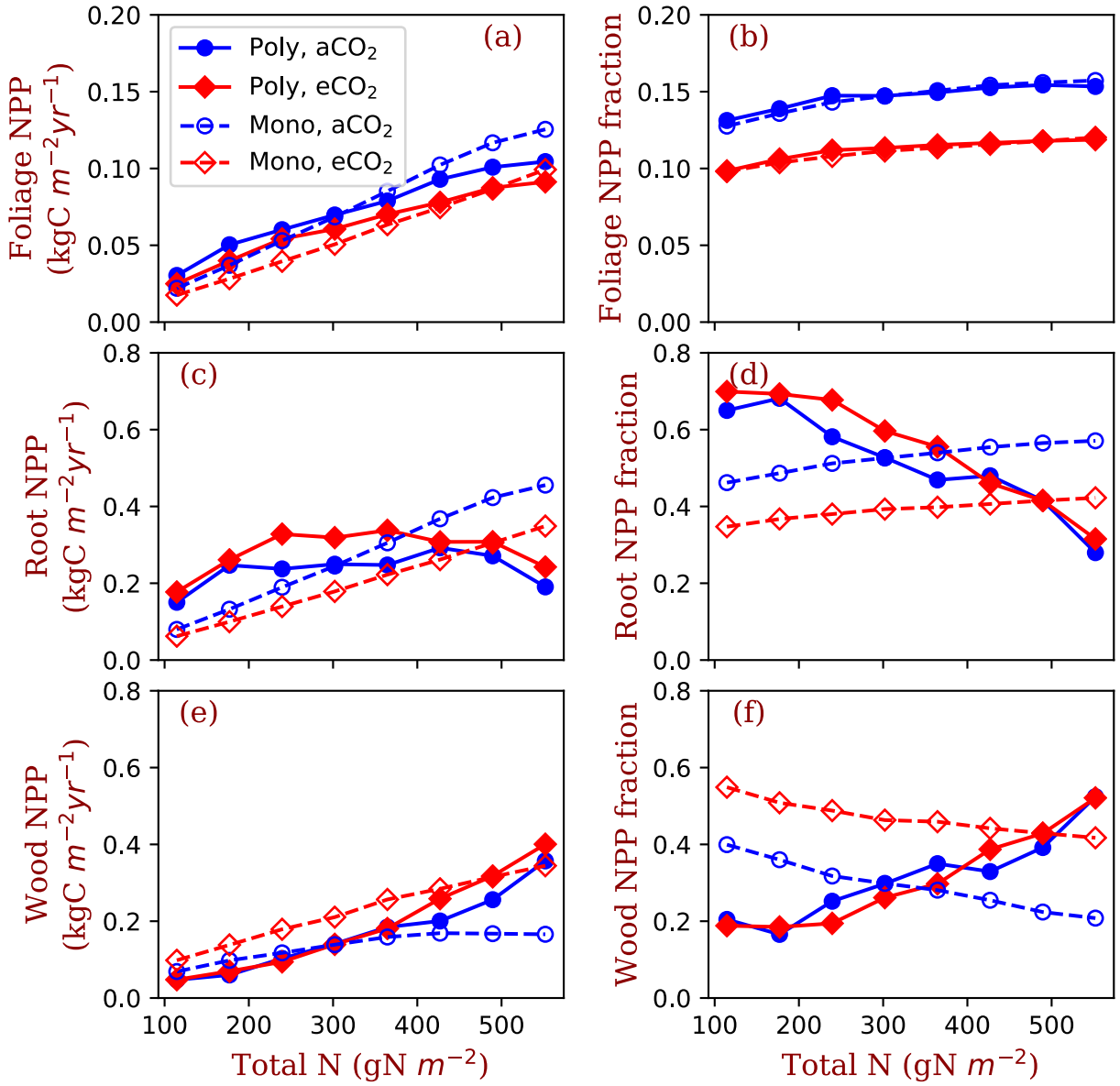

Figure 6 Allocation to leaves, fine roots, and wood tissues of the competition and monoculture runs at the eight total nitrogen levels and two CO_2 concentrations (aCO_2: 380 ppm; eCO_2: 580 ppm). The panels a, c, and e show the NPP allocated to the tissues and the panels b, d, and f show the fractions of the allocation in total NPP. The closed symbols with solid line represent polyculture runs (poly.). The open symbols with dashed lines represent monoculture runs (only φ_{RL}=4 shown in this figure). φ_{RL} is the fixed ratio of fine root area to leaf area of a particular strategy.

453 Fine root NPP does not significantly change with total nitrogen in polyculture runs,
454 whereas it increases monotonically with increasing nitrogen in monoculture runs (Fig. 6: c).
455 Elevated [CO_2] increases fine root allocation at low nitrogen in polyculture runs but decreases
456 root allocation irrespective of nitrogen in monoculture runs (Fig. 6: c). The fraction of NPP
457 allocated to fine roots decreases with nitrogen at both CO_2 concentrations in polyculture runs but
458 it increases slightly in monoculture runs (Fig. 6: d). In monoculture runs, elevated CO_2 reduces
459 the fraction of NPP allocated to fine roots at all nitrogen levels. In polyculture runs, fractional
460 allocation to fine roots increases at elevated [CO_2] when ecosystem total nitrogen is low (e.g.,
461 114.5 - 302 g N m^{-2}) and decrease at elevated [CO_2] when ecosystem total nitrogen is high (e.g.,
462 364-552 g N m^{-2}).

463 In the reverse of the fine root response, NPP allocation to woody tissues increases with
464 total nitrogen in both competition and monoculture runs (Fig. 6: e). In polyculture runs, the
465 fraction of allocation to woody tissues decreases at elevated [CO_2] when ecosystem total
466 nitrogen is low (e.g., 114 – 245 g N m^{-2}) and increases at elevated [CO_2] when ecosystem total
467 nitrogen is high (e.g., 302 – 552 g N m^{-2}).

468

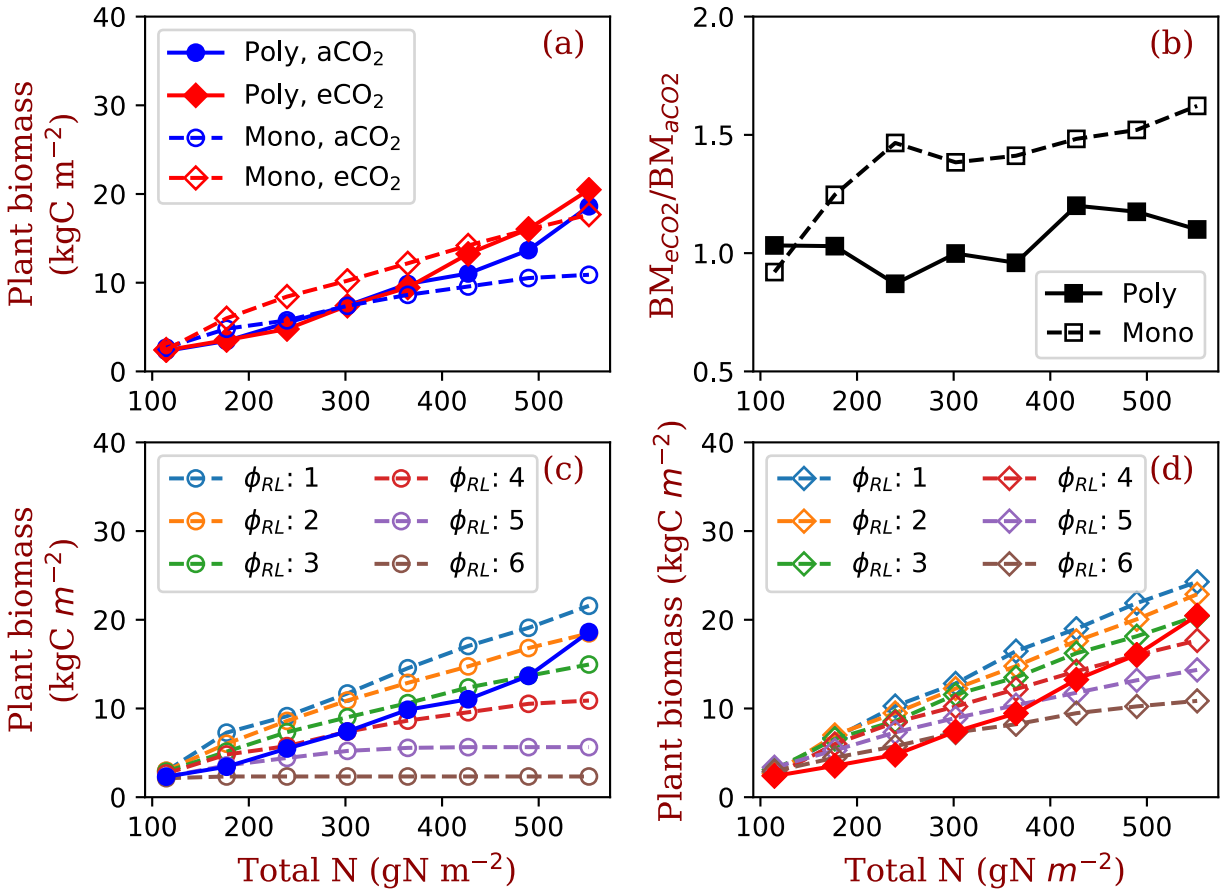

469

470 **Figure 7 Plant biomass responses to elevated [CO_2] and nitrogen**

471 Panel a shows the equilibrium plant biomass (means of simulated plant biomass from model run
472 year 1400 to 1800) in polyculture runs and monoculture runs (only φ_{RL}=4 shown as an example).
473 Panel b shows the ratio of simulated plant biomass at elevated [CO_2] to ambient [CO_2] for both
474 competition and monoculture runs. Panels c and d show the comparisons with monoculture runs
475 with φ_{RL} increasing from 1 to 6 at ambient (c) and elevated [CO_2] (d). The closed symbols with
476 solid line represent polyculture runs. The open symbols with dashed lines represent monoculture
477 runs (φ_{RL} ranges from 1 to 6). φ_{RL} is the fixed ratio of fine root area to leaf area of a particular
478 strategy. aCO_2: 380 ppm; eCO_2: 580 ppm.

479

As a result of the changes in competitively-optimal φ_{RL}, plant biomass increases dramatically with ecosystem nitrogen in polyculture runs compared with that in monoculture runs (Fig. 7: a). The effects of elevated [CO_2] on plant biomass increase with nitrogen in polyculture runs but are constant overall in monoculture runs (Fig. 7: b). Compared with the full spread of monoculture runs with φ_{RL} ranging from 1 to 6, polyculture runs have high root allocation at low nitrogen and low root allocation at high nitrogen due to changes in the dominant competitive allocation strategy, which amplifies plant biomass responses to elevated [CO_2] with increasing nitrogen (Fig. 7: c and d).

4 Discussion

Our simulations show that the responses of individual plants to elevated [CO_2] can be significantly changed by explicit inclusion of competition processes. Here, the major tradeoff for light- and N-limited trees is the relative allocation between stems and fine roots (Dybzinski et al. 2011). Although the wood allocation (and thus carbon sequestration potential) of every PFT used in this study increases under elevated [CO_2] at all nitrogen levels (e.g. Fig. 6e dashed lines), only those PFTs that allocate more to fine roots (with lower carbon sequestration potential) can survive competition under elevated [CO_2] (Fig. 6c solid lines). Put together, explicit inclusion of competition processes reduces the expected increase in biomass (and thus carbon sequestration potential) under elevated [CO_2] compared with simulations that do not include competition processes (Fig. 7b).

Since there is a lack of direct observations or experiments to quantitatively validate the long-term patterns predicted by our model, we did not calibrate it to fit observations at Harvard Forest. In the following section, we analyze the model processes in detail and validate our

503 modeling approach by comparing the general patterns from observations and experiments with
504 model predictions. These comparisons also shed light on the modeling of allocation and
505 vegetation responses to elevated [CO_2].

506

507 **4.1 Mechanisms of game-theoretic allocation modeling and simulation results validation**

508 In our model, the allocation of carbon and nitrogen within an individual tree is based on
509 allometric scaling (Eq. 2), functional relationships (Eq. 3), and optimization of resource usage
510 (Eqs. 6 and 7). Generally, the allometric scaling relationships define the maximum leaf and fine
511 root surface area at a given tree size, and the functional relationships define the ratios of leaf area
512 to sapwood cross-sectional area and fine root surface area. These rules are commonly used in
513 ecosystem models (Franklin et al., 2012) and have been shown to generate reasonable
514 predictions (De Kauwe et al., 2014; Valentine and Mäkelä, 2012). These rules implicitly define
515 the priority of allocation to leaves and fine roots but allow for structurally-unlimited stem growth
516 when resources (carbon and nitrogen in this study) are available (i.e., the remainder goes to
517 stems after leaf and fine root growth).

518 We used a tuning parameter, maximum leaf and fine root allocation, $f_{LFR,max}$, to constrain
519 the maximum allocation to leaves and fine roots in order to maintain a minimum growth rate of
520 wood in years of low productivity. This is consistent with wood growth patterns in temperate
521 trees, where new wood tissues must be continuously produced (especially early in the growing
522 season) to maintain the functions of tree trunks and branches (Cuny et al., 2012; Michelot et al.,
523 2012; Plomion et al., 2001). This parameter does not change the fact that leaves and fine roots
524 are the priority in allocation, since allocation ratios to stems are around 0.4~0.7 in temperate
525 forests (Curtis et al., 2002; Litton et al., 2007). With a value of 0.85, $f_{LFR,max}$ only seldom affects

526 the overall carbon allocation ratios of leaves, fine roots, and stems and still maintains wood grow
527 in years of low productivity. If $f_{LFR,max} = 1$ (i.e., the highest priority for leaf and fine root
528 growth), simulated trunk radial growth would have unreasonably high interannual variation
529 because leaf and fine root growth would use all carbon to approach to their targets, leaving
530 nothing for stems in some years of low productivity.

531 The simulation of competition for light and soil resources is based on two fundamental
532 mechanisms: 1) competition for light is based on the height of trees according to the PPA model,
533 which assumes trees have perfectly plastic crown to capture light via stem (trunk) and branch
534 phototropism (Strigul et al., 2008); and 2) individual N uptake is linearly dependent on the fine
535 root surface area of an individual tree relative to that of its neighbors (Dybzinski et al., 2019;
536 McMurtrie et al., 2012; Weng et al., 2017). These two mechanisms define an allocational
537 tradeoff between wood and fine roots for carbon and N investment in different CO_2
538 concentrations and nitrogen environments. Including explicit competition for these resources to
539 determine the dominant strategies results in very different predicted allocation patterns – and
540 thus ecosystem level responses – than those of strategies in the absence of competition. For
541 example, fractional wood allocation increases with increasing nitrogen availability under
542 competitive allocation but decreases – *the opposite qualitative response* – under a fixed strategy
543 (Fig. 6: f). Consequently, equilibrium plant biomass is predicted to increase much more with
544 increasing nitrogen availability under a competitive strategy (Fig. 4: c, d). In nature, the effects
545 of competition on dominant plant traits may occur through species replacement or community
546 assembly (akin to the mechanism in our model) (e.g., Douma et al., 2012), but it may also occur
547 through adaptive plastic responses or in-place sub-population evolution of ecotypes (Grams and
548 Andersen, 2007; McNickle and Dybzinski, 2013; Smith et al., 2013).

549 Generally, the predictions from competitively-optimal allocation strategies predicted by
550 our model can be found in large scale forest censuses and site-level experiments, such as: 1) high
551 nitrogen environments (i.e., productive environments) favor high wood allocation and low root
552 allocation (Litton et al., 2003; Poorter et al., 2012); 2) elevated [CO_2] increases root allocation
553 (Drake et al., 2011; Iversen, 2010; Jackson et al., 2009; Nie et al., 2013; Smith et al., 2013); 3)
554 low nitrogen availability limits vegetation biomass responses to elevated [CO_2] as a result of
555 high root allocation or root exudation (Jiang et al., 2019a; Norby and Zak, 2011); and 4)
556 increases in vegetation biomass at elevated [CO_2] are largely due to high wood allocation (Norby
557 and Zak, 2011; Walker et al., 2019). These predictions emerged from the fundamental
558 assumptions of our model without tuning parameters to fit the data, providing some confidence
559 in the robustness of our approach.

560 The literature on experimental responses of plant community to elevated [CO_2] shows
561 that the responses vary with site characteristics, forest composition, stand age, plant
562 physiological responses, and soil microbial feedbacks. For example, in Duke Free Air CO_2
563 Enhancement (FACE) experiment, where the major trees are loblolly pine (*Pinus taeda*),
564 increases in root production at elevated [CO_2] stimulated increased nitrogen supply that allowed
565 the forest to sustain higher productivity (Drake et al., 2011). However, in Oak Ridge FACE,
566 where the major trees are sweetgum (*Liquidambar styraciflua*), increased fine-root production
567 under elevated [CO_2] did not result in increased net nitrogen mineralization and increases in root
568 production declined after eight years of CO_2 enhancement (Iversen, 2010; Norby and Zak, 2011).
569 In EucFACE, where the major trees are *Eucalyptus tereticornis* and the soil is infertile, trees
570 significantly increased their root exudation under limited nutrient supplies but had no significant
571 increase in biomass in response to elevated [CO_2] (Jiang et al., 2019a). The BangorFACE

572 experiment (Smith et al., 2013) found that interspecific competition (*Alnus glutinosa*, *Betula*
573 *pendula* and *Fagus sylvatica*) resulted in greater increases in root biomass at elevated [CO_2].
574 Leaf area index (LAI) responses to elevated [CO_2] are also highly varied. As summarized by
575 Norby and Zak (2011), low LAI (in this case, open canopy) sites showed significant increases in
576 LAI and high LAI (in this case, closed canopy) sites showed low increases or even decreases in
577 LAI. They concluded that LAI in closed-canopy forests is not responsive to elevated [CO_2]
578 (Norby et al., 2003; Norby and Zak, 2011).

579 The nature of developing a model with generic assumptions and balanced processes
580 reduces its capability to predict all of these responses. For example, plants have a variety of
581 physiological mechanisms to deal with excessive carbon supply when plant demand (i.e., "sink")
582 is relatively low (Fatichi et al., 2019; Körner, 2006), such as down-regulating leaf photosynthesis
583 rate by the accumulated assimilates (Goldschmidt and Huber, 1992) or respiring excessive
584 carbohydrates to regenerate substrates for photosynthesis (Atkin and Macherel, 2009). But these
585 mechanisms are short-term physiological responses (minutes to hours, sometimes days) for
586 plants in situations of temporary nitrogen shortage, high irradiation, or drought stress. It is not
587 "economically" sustainable in an infertile environment to maintain highly productive leaves but
588 to often suppress their photosynthesis or respire a large portion of their assimilated carbon.

589 Root exudation is a critical process for plants. It can stimulate soil organic matter
590 decomposition and nitrogen mineralization to facilitate soil nitrogen supply at the expense of
591 carbon (Cheng, 2009; Cheng et al., 2014; Drake et al., 2011; Phillips et al., 2011). The process of
592 root exudation has been adopted by many models to couple with microbial processes in the
593 determination of soil organic matter decomposition (Sulman et al., 2014; Wieder et al., 2014,
594 2015). Some carbon-only models, e.g., LM3 (Shevliakova et al., 2009), the parent model of this

595 one, and TECO (Luo et al., 2001), incorporate root exudation to put extra carbon into the soil in
596 order to avoid down-regulating canopy photosynthesis or overestimating vegetation biomass,
597 both of which had been tuned against data. However, in a demographic competition model like
598 this one, when the microbial activities are not fully coupled and the nitrogen in soil is assumed
599 fully accessible by roots of all individuals, individual plants cannot reap a reward from root
600 exudation as they do in nature. Therefore, root exudation is not a competitive strategy in the
601 system defined by the assumptions of this model.

602 Since the purpose of this study is to explore long-term ecological strategies in different
603 but relatively stable environments, we did not include these processes, especially since they
604 present additional challenges in balancing the complexity of the tradeoffs between modeled
605 demographic processes and plant traits. However, the lack of these processes does limit the
606 predictions of instantaneous responses to variation in environmental conditions or resource
607 supply and possibly of some long-term vegetation characteristics as well. For example, our
608 model predicts reduced LAI under nitrogen limitation (Fig. S11) based on first principles, but it
609 is incidentally the only mechanism that reduces the whole-canopy photosynthesis rate in our
610 model. There are mechanisms that increase nitrogen use efficiency at the expense of carbon by
611 increasing LMA and therefore leaf longevity to maintain high LAI and high canopy-level
612 photosynthesis rates (Aerts, 1995, 1999; Aerts and Chapin, 1999; Givnish, 2002). We did not
613 include these mechanisms in our simulations, although they are well-developed in this model
614 (Weng et al. 2017), because we wished to focus on the strategy of allocation. The clear
615 descriptions of our model's assumptions, its traceable processes, and inclusion of the tradeoffs
616 involved in aboveground and belowground competition provide a useful benchmark from which
617 to incorporate additional mechanisms and tradeoffs.

618

619 **4.2 Root overproliferation vs. wood allocation**

620 The allocation strategy that maximizes site vegetation biomass allocates very little to fine
621 roots (Figs. 3 and S1). In contrast, the competitively optimal strategy allocates more carbon to
622 fine roots, termed "fine-root overproliferation" in the literature (Gersani et al., 2001; McNickle
623 and Dybzinski, 2013; O'Brien et al., 2005). It is the result of a competitive "arms race": while
624 increasing fine root area under elevated [CO_2] does not result in more nitrogen for an individual,
625 failing to do so would cede some of that individual's nitrogen to its neighbors. Because most
626 nitrogen uptake is via mass flow and diffusion (Oyewole et al., 2017) and because both of these
627 mechanisms depend on sink strength, individuals with *relatively* greater fine root mass than their
628 neighbors take a greater share of nitrogen, as was recently demonstrated empirically (Dybzinski
629 et al., 2019; Kulmatiski et al., 2017). Thus, fine roots may overproliferate for competitive
630 reasons relative to lower optimal fine root mass in the hypothetical absence of an evolutionary
631 history of competition (Craine, 2006; McNickle and Dybzinski, 2013). This may also explain
632 why root C:N ratio is highly variable (Dybzinski et al., 2015; Luo et al., 2006; Nie et al., 2013): a
633 high density of fine roots in soil may be more important than the high absorption ability of a
634 single root in competing for soil nitrogen in the usually low mineral nitrogen soils.

635 Root overproliferation is still controversial in experiments. For example, Gersani et al.
636 (2001) and O'Brien (2005) found that competing plants generated more roots than those
637 growing in isolation; whereas McNickle and Brown (2014) found that competing plants
638 generated comparable roots to those growing in isolation. Compared to modeled roots, real roots
639 are far more adaptive and complex at modifying their growth patterns in response to soil nutrient
640 and water dynamics (Hodge, 2009). The root growth strategies in response to competition also

641 vary with species (Belter and Cahill, 2015). The mechanisms of self-recognition of inter- and
642 intra- roots also can lead to varied behavior of root growth (Chen et al., 2012). However, all of
643 the aforementioned studies considered only *plastic* root overproliferation, where individuals
644 produce more roots in the presence of other individuals than they do in isolation, analogous to
645 stem elongation of crowded seedlings (Dudley and Schmitt, 1996). A portion of root
646 overproliferation may also be *fixed*, analogous to trees that still grow tall even when grown in
647 isolation. Dybzinski et al. (2019) showed that plant community nitrogen uptake rate was
648 independent of fine root mass in seedlings of numerous species, suggesting a high degree of
649 fixed fine root overproliferation. To improve root competition models, more detailed
650 experiments that control root growth should be conducted to quantify the marginal benefits of
651 roots in isolated, monoculture, and polyculture environments.

652 At high soil nitrogen, height-structured competition for light (also a game-theoretic
653 response, Falster and Westoby, 2003; Givnish, 1982) prevails, and trees with greater *relative*
654 allocation to trunks prevail. The balance between these two competitive priorities (fine roots vs.
655 stems) can be observed in our model predictions as a shift from fine root allocation to wood
656 allocation as soil nitrogen increases. The increases in the critical height (i.e. the context-
657 dependent height of the shortest tree in canopy layer in the PPA) from low nitrogen to high
658 nitrogen indicates a shift from the importance of competition for soil nitrogen to the importance
659 of competition for light as ecosystem nitrogen increases (Fig. S6). Because the most competitive
660 type shifts from high fine root allocation to low fine root allocation as ecosystem total nitrogen
661 increases, increases in NPP and plant biomass across the nitrogen gradient are greater than the
662 increases in NPP and plant biomass assuming allocational strategies in the absence of
663 competition (Fig. 3). This greatly reduces the carbon cost of belowground competition as

ecosystem total nitrogen increases. The decrease in the fraction of NPP allocated to leaves at elevated [CO_2] (Fig. 6: b)occurs because of increases in total NPP and nearly constant absolute NPP allocation to foliage (Fig. 6: a).

4.3 Model complexity and uncertainty

Compared with the conventional pool-based vegetation models that use pools and fluxes to represent plant demographic processes at a land simulation unit (e.g., grid or patch), VDMs add two more layers of complexity. The first is the inclusion of stochastic birth and mortality processes of individuals (i.e., demographic processes). These processes allow the models to predict population dynamics and transient vegetation structure, such as size-structured distribution and crown organization (e.g., Moorcroft et al., 2001; Strigul et al., 2008). With changes in vegetation structure, allocation and mortality rates can change, generating a different carbon storage accumulation curve compared with those predicted by pool-based models where vegetation structure is not explicitly represented (e.g., Weng et al., 2015). The second is the simulated shift in dominant plant traits during succession due to the shifting of competitive outcomes among different PFTs, which changes the allocation between fast- and slow-turnover pools and thus the parameters of allocation and the residence time of carbon in the ecosystem.

Together, these mechanisms may alter long-term predictions of terrestrial carbon cycling due to changes in PFT-based parameters (Dybzinski et al., 2011; Farrior et al., 2013; Weng et al., 2015). As described in Introduction, current pool-based models can be described by a linear system of equations characterized by the key parameters of allocation, residence time, and transfer coefficients (Eq. 1) with the rigid assumption of unchangeable plant types (Luo et al., 2012; Xia et al., 2013). In VDMs however, allocation, residence time, leaf traits, phenology,

687 mortality, plant forms, and their responses to climate change are all strategies of competition
688 whose success varies with the environmental conditions and the traits of the individuals they are
689 competing against.

690 Many tradeoffs between plant traits can shift in response to environmental and biotic
691 changes, limiting the applicability of varying a single trait, as we have in this study. For example,
692 allocation, leaf traits, mycorrhizal types, and nitrogen fixation can all change with ecosystem
693 nitrogen availability (Menge et al., 2017; Ordoñez et al., 2009; Phillips et al., 2013; Vitousek et
694 al., 2013). The unrealistic effects of model simplification can be corrected by adding important
695 tradeoffs that are missing. For example, the positive feedback between root allocation and SOM
696 decomposition plays a role in mitigating the effects of tragedies of the commons of root over-
697 proliferation (e.g., Gersani et al., 2001; Zea-Cabrera et al., 2006) due to a negative feedback
698 induced by root turnover. High root allocation increases the decomposition rate of SOM and the
699 supply of mineral nitrogen because of the high turnover rate of root litter, which favors a strategy
700 of high wood allocation and reduces the competitive optimal fine root allocation. This negative
701 feedback indicates that the model structure is flexible and that we can incorporate correct
702 mechanisms step by step to improve model prediction skills. Testing single strategies is still a
703 necessary step to improving our understanding of the system and prediction skills of the models,
704 though it could lead to unrealistic responses sometimes.

705 We conducted simulations only at one site for the purpose of exploring the general
706 patterns of competitively optimal allocation strategies and their responses to elevated [CO_2] at
707 different nitrogen availabilities. We can speculate about shifts in the competitively optimal
708 allocation strategy in different forest biomes by considering the effects of temperature on soil
709 nitrogen supply via the SOM's decomposition rate and its positive effect on net nitrogen

710 mineralization. For example, the SOM decomposition rate is usually high in warm regions and
711 low in cold regions (Davidson and Janssens, 2006) assuming there are no water limitations and
712 SOM is equilibrated with carbon input. According to our model, allocation to roots is high in low
713 nitrogen supply conditions (cold regions) and low in high nitrogen supply conditions (warm
714 regions). This pattern can be found from temperate to boreal forest zones (Cairns et al., 1997;
715 Gower et al., 2001; Reich et al., 2014; Zadworny et al., 2016). Temperature also alters NPP, i.e.,
716 carbon supply: as temperature goes down, NPP decreases and nitrogen demand decreases,
717 alleviating nitrogen limitation and leading to shifts of allocation to stems. So, the differences in
718 temperature effects on photosynthesis and SOM decomposition will determine competitive
719 allocation strategy. Since SOM decomposition is more sensitive to temperature than gross
720 primary production is at long-temporal and large-spatial scales (Beer et al., 2010; Carey et al.,
721 2016; Crowther et al., 2016), our model suggests that allocation will shift to wood in a warming
722 world. Whether the carbon stored in that wood is enough to offset the carbon released from
723 increasing soil respiration is a critical question.

724 Water is also a critical factor affecting allocation and its responses to elevated [CO_2].
725 Low soil moisture usually leads to high allocation to roots (Poorter et al., 2012). Elevated CO_2
726 can reduce transpiration (as found in our study as well, Fig S7) and therefore increase soil
727 moisture, resulting in increases in allocation to stems and aboveground biomass (Walker et al.,
728 2019). A game-theoretic modeling study using the PPA framework shows that the competitively
729 optimal allocation strategy shifts to high wood allocation at elevated [CO_2] in environments with
730 water limitation (Farrior et al., 2015). This is opposite to the elevated [CO_2] effects on allocation
731 in nitrogen-limited environments as simulated in this study. According to field experiments, fine
732 root allocation is more responsive to nitrogen changes than it to soil moisture changes (Canham

et al., 1996; Poorter et al., 2012). Poorter et al. (2012) attribute the mechanisms to the optimal strategies in response to the relative stable nitrogen supply and stochastic water input in soil. The vertical distribution of roots and the contributions of roots in different layers to water and nitrogen uptake also suggest that the uptake of soil nutrients are dominant in shaping root system architecture (Chapman et al., 2012; Morris et al., 2017), though root growth and turnover are flexible and sensitive to nitrogen and water supply (Deak and Malamy, 2005; Linkohr et al., 2002; Pregitzer et al., 1993).

We found that model predictions can differ significantly in response to seemingly-small variations in basic assumptions or quantitative relationships. For example, our model predicts that the ratio of plant biomass under elevated [CO_2] relative to plant biomass under ambient [CO_2] should increase with increasing nitrogen due to the shift of carbon allocation from fine roots to woody tissues. In contrast, the analytic model of Dybzinski *et al*. (2015) predicts that the ratio of plant biomass under elevated [CO_2] relative to plant biomass under ambient [CO_2] should be largely independent of total nitrogen because of an increasing shift in carbon allocation from long-lived, low-nitrogen wood to short-lived, high-nitrogen fine roots under elevated [CO_2] and with increasing nitrogen. This significant difference between these two predictions traces back to differences in how fine root stoichiometry is handled in the two models. In the model of Dybzinski *et al*. (2015), the fine root C:N ratio is flexible and the marginal nitrogen uptake capacity per unit of carbon allocated to fine roots depends on its nitrogen concentration. Like the model presented here, the model of Dybzinski *et al*. (2015) predicts decreasing fine root mass with increasing nitrogen availability. *Unlike* the model presented here (which has constant fine root nitrogen concentration), the model of Dybzinski et al. (2015) predicts increasing fine root nitrogen concentration with increasing nitrogen availability. As a result, there is less nitrogen to

allocate to wood as nitrogen increases in the model of Dybzinski *et al*. (2015) than there is in the model presented here. These countervailing factors even out the ratio of plant biomass under elevated [CO_2] relative to plant biomass under ambient [CO_2] across the nitrogen gradient in Dybzinski *et al*. (2015), whereas their absence amplifies this ratio with increasing nitrogen in the model presented here. Our ability to diagnose and understand this discrepancy highlights the utility of deploying closely-related analytical and simulation models (Weng et al., 2017).

4.4 Common principles for allocation modeling and implications

As shown in model inter-comparison studies, the mechanisms of modeling allocation differ very much, leading to high variation in their predictions (e.g., De Kauwe et al. 2014). Calibrating model parameters to fit data may not increase model predictive skill because data are often also highly variable. Franklin et al. (2012) suggest that in order to build realistic and predictive allocation models, we should correctly identify and implement fundamental principles. Our model predicts similar patterns to those predicted by the model of Valentine and Mäkelä (2012), which has very different processes of plant growth and allocation. However, these two models share fundamental principles, including 1) evolutionary- or competitive-optimization, 2) capped leaves and fine roots at given tree sizes, 3) structurally unlimited stem allocation (i.e., optimizing carbon use) because the woody tissues can serve as unlimited sink for surplus carbon, and 4) height-structure competition for light and root-mass-based competition for soil resources. The principles 2 and 3 are commonly used in models (De Kauwe et al., 2014; Jiang et al., 2019b). However, the different rules of implementing them (e.g., allometric equation, functional relationships, etc.) lead to highly varied predictions (as shown in De Kauwe et al., 2014), though model formulations may be very similar.

779 In competitively-optimal models, such as this study and also Valentine and Mäkelä (2012),
780 the competition processes generate similar emergent patterns by selecting those that can survive
781 in competition, regardless the details of those differences. The competition processes also make
782 the details of allocation settings for a single PFT and their direct responses to elevated [CO_2] less
783 important, because competition processes will select out the most competitive strategy from
784 diverse strategies in response to changes in [CO_2] and nitrogen. Our study and Valentine and
785 Mäkelä (2012), posit a fundamental tradeoff between light competition and nitrogen competition
786 via allocation based on insights gained from simpler models (e.g., Dybzinski et al., 2015; Mäkelä
787 et al., 2008) for predicting allocation as an emergent property of competition. One advantage of
788 building a model in this way is that the vegetation dynamics are predicted from first principles,
789 rather than based on the correlations between vegetation properties and environmental
790 conditions. With these first principles, the models can produce reasonable predictions, though the
791 details of physiological and demographic processes vary among models.

792 For vegetation models designed to predict the effects of climate change, the important
793 operational distinction is that the fundamental rules cannot or will not change as climate changes.
794 Nor, presumably, will the underlying ecological and evolutionary processes change as climate
795 changes. The emergent properties can change as climate changes however, and the models built
796 on the "scale-appropriate" unbreakable constraints and ecological and evolutionary processes
797 will be able to accurately predict changes in emergent ecosystem properties (Weng et al., 2017).
798 In our opinion, the scientific effort to build better models is better served by understanding
799 unrealistic predictions than by "fixing" them with unreliable mechanisms when there is a lack of
800 data or theory to make them consistent with observations. Validating assumptions and initial
801 responses are critical, and the long-term responses can be validated via spatial patterns.

This modeling approach also demands improvement in model validation and benchmarking systems (Collier et al., 2018; Hoffman et al., 2017). As shown in this study, allocation responses to elevated CO_2 at different nitrogen levels in monoculture runs are opposite to those in competitive-allocation runs. For example, in monoculture runs, elevated [CO_2] increases wood allocation and decreases fine root allocation at low nitrogen; whereas in competitive-allocation runs elevated [CO_2] leads to low wood allocation and high fine root allocation. Simply calibrating our model against short-term observational data may improve the agreement with observations but would not change the model's predictions because the model's predictions emerge from its fundamental assumptions.

5 Conclusions

Our study illustrates that including the competition processes for light and soil resources in a game-theoretic vegetation demographic model can substantially change the prediction of the contribution of ecosystems to the global carbon cycle. Allowing the model to explicitly track the competitive allocation strategies can generate significantly different ecosystem-level predictions (e.g., biomass and ecosystem carbon storage) than those of strategies in the absence of explicit competition. Building such a model requires differentiating between the unbreakable tradeoffs of plant traits and ecological processes from the emergent properties of ecosystems. Drawing on insights from closely-related analytical models to develop and understand more complicated simulation models seems, to us, indispensable. Evaluating these models also requires an updated model benchmarking system that includes the metrics of competitive plant traits during the development of ecosystems and their responses to global change factors.

Acknowledgements

This work was supported by NASA Modeling, Analysis, and Prediction (MAP) Program (NNH16ZDA001N-MAP), USDA Forest Service Northern Research Station (Agreement 13-JV-11242315-066) and Princeton Environment Institute. C.E.F acknowledges support from the University of Texas at Austin.

Codes and data availability

The codes of the BiomeE model are available at GitHub:

https://github.com/wengensheng/BiomeESS

The simulated data from simulation experiments and Python scripts used in this study will be made publicly available at the publish of this paper.

Reference

Aber, J. D., Magill, A., Boone, R., Melillo, J. M. and Steudler, P.: Plant and Soil Responses to Chronic Nitrogen Additions at the Harvard Forest, Massachusetts, Ecological Applications, 3(1), 156–166, doi:10.2307/1941798, 1993.

Aerts, R.: The advantages of being evergreen, Trends in ecology & evolution, 10(10), 402–407, 1995.

Aerts, R.: Interspecific competition in natural plant communities: mechanisms, trade-offs and plant-soil feedbacks, Journal of Experimental Botany, 50(330), 29–37, 1999.

Aerts, R. and Chapin, F. S.: The Mineral Nutrition of Wild Plants Revisited: A Re-evaluation of Processes and Patterns, in Advances in Ecological Research, vol. 30, edited by A. H. Fitter and D. G. Raffaelli, pp. 1–67, Academic Press., 1999.

Arora, V. K. and Boer, G. J.: A parameterization of leaf phenology for the terrestrial ecosystem component of climate models, Global Change Biology, 11(1), 39–59, doi:10.1111/j.1365-2486.2004.00890.x, 2005.

Atkin, O. K. and Macherel, D.: The crucial role of plant mitochondria in orchestrating drought tolerance, Ann Bot, 103(4), 581–597, doi:10.1093/aob/mcn094, 2009.

Barr, A. G., Ricciu, D. M., Schaefer, K., Richarson, A., Agarwal, D., Thornton, P. E., Davis, K., Jackson, B., Cook, R. B., Hollinger, D. Y., Van Ingen, C., Amiro, B., Andrews, A., Arain, M. A., Baldocchi, D., Black, T. A., Bolstad, P., Curtis, P., Desai, A., Dragoni, D., Flanagan, L., Gu, L., Katul, G., Law, B. E., Lafleur, P. M., Margolis, H., Matamala, R., Meyers, T., McCaughey, J. H., Monson, R., Munger, J. W., Oechel, W., Oren, R., Roulet, N. T., Torn, M. and Verma, S. B.: NACP Site: Tower Meteorology, Flux Observations with Uncertainty, and Ancillary Data, , doi:10.3334/ornldaac/1178, 2013.

Beer, C., Reichstein, M., Tomelleri, E., Ciais, P., Jung, M., Carvalhais, N., Rodenbeck, C., Arain, M. A., Baldocchi, D., Bonan, G. B., Bondeau, A., Cescatti, A., Lasslop, G., Lindroth, A., Lomas, M., Luyssaert, S., Margolis, H., Oleson, K. W., Roupsard, O., Veenendaal, E., Viovy, N., Williams, C., Woodward, F. I. and Papale, D.: Terrestrial Gross Carbon Dioxide Uptake: Global Distribution and Covariation with Climate, Science, 329(5993), 834–838, doi:10.1126/science.1184984, 2010.

Belter, P. R. and Cahill, J. F.: Disentangling root system responses to neighbours: identification of novel root behavioural strategies, AoB PLANTS, 7, plv059, doi:10.1093/aobpla/plv059, 2015.

Bloom, A. A., Exbrayat, J.-F., van der Velde, I. R., Feng, L. and Williams, M.: The decadal state of the terrestrial carbon cycle: Global retrievals of terrestrial carbon allocation, pools, and residence times, Proceedings of the National Academy of Sciences, 113(5), 1285–1290, doi:10.1073/pnas.1515160113, 2016.

872 Cairns, M. A., Brown, S., Helmer, E. H. and Baumgardner, G. A.: Root biomass allocation in the
873 world's upland forests, Oecologia, 111(1), 1–11, doi:10.1007/s004420050201, 1997.

874 Canham, C. D., Berkowitz, A. R., Kelly, V. R., Lovett, G. M., Ollinger, S. V. and Schnurr, J.: Biomass
875 allocation and multiple resource limitation in tree seedlings, Canadian Journal of Forest
876 Research-Revue Canadienne De Recherche Forestiere, 26(9), 1521–1530, doi:10.1139/x26-171,
877 1996.

878 Cannell, M. G. R. and Dewar, R. C.: Carbon Allocation in Trees: a Review of Concepts for
879 Modelling, in Advances in Ecological Research, vol. 25, pp. 59–104, Elsevier., 1994.

880 Carey, J. C., Tang, J., Templer, P. H., Kroeger, K. D., Crowther, T. W., Burton, A. J., Dukes, J. S.,
881 Emmett, B., Frey, S. D., Heskel, M. A., Jiang, L., Machmuller, M. B., Mohan, J., Panetta, A. M.,
882 Reich, P. B., Reinsch, S., Wang, X., Allison, S. D., Bamminger, C., Bridgham, S., Collins, S. L., de
883 Dato, G., Eddy, W. C., Enquist, B. J., Estiarte, M., Harte, J., Henderson, A., Johnson, B. R., Larsen,
884 K. S., Luo, Y., Marhan, S., Melillo, J. M., Peñuelas, J., Pfeifer-Meister, L., Poll, C., Rastetter, E.,
885 Reinmann, A. B., Reynolds, L. L., Schmidt, I. K., Shaver, G. R., Strong, A. L., Suseela, V. and
886 Tietema, A.: Temperature response of soil respiration largely unaltered with experimental
887 warming, Proceedings of the National Academy of Sciences, 113(48), 13797–13802,
888 doi:10.1073/pnas.1605365113, 2016.

889 Chapman, N., Miller, A. J., Lindsey, K. and Whalley, W. R.: Roots, water, and nutrient
890 acquisition: let's get physical, Trends in Plant Science, 17(12), 701–710,
891 doi:10.1016/j.tplants.2012.08.001, 2012.

892 Chen, B. J. W., During, H. J. and Anten, N. P. R.: Detect thy neighbor: Identity recognition at the
893 root level in plants, Plant Science, 195, 157–167, doi:10.1016/j.plantsci.2012.07.006, 2012.

894 Cheng, W.: Rhizosphere priming effect: Its functional relationships with microbial turnover,
895 evapotranspiration, and C-N budgets, Soil Biology & Biochemistry, 41(9), 1795–1801,
896 doi:10.1016/j.soilbio.2008.04.018, 2009.

897 Cheng, W., Parton, W. J., Gonzalez-Meler, M. A., Phillips, R., Asao, S., McNickle, G. G., Brzostek,
898 E. and Jastrow, J. D.: Synthesis and modeling perspectives of rhizosphere priming, New
899 Phytologist, 201(1), 31–44, doi:10.1111/nph.12440, 2014.

900 Collier, N., Hoffman, F. M., Lawrence, D. M., Keppel-Aleks, G., Koven, C. D., Riley, W. J., Mu, M.
901 and Randerson, J. T.: The International Land Model Benchmarking (ILAMB) System: Design,
902 Theory, and Implementation, Journal of Advances in Modeling Earth Systems, 10(11), 2731–
903 2754, doi:10.1029/2018MS001354, 2018.

904 Compton, J. E. and Boone, R. D.: Long-Term Impacts of Agriculture on Soil Carbon and Nitrogen
905 in New England Forests, Ecology, 81(8), 2314, doi:10.2307/177117, 2000.

906 Craine, J. M.: Competition for Nutrients and Optimal Root Allocation, Plant and Soil, 285(1–2),
907 171–185, doi:10.1007/s11104-006-9002-x, 2006.

908 Crowther, T. W., Todd-Brown, K. E. O., Rowe, C. W., Wieder, W. R., Carey, J. C., Machmuller, M.
909 B., Snoek, B. L., Fang, S., Zhou, G., Allison, S. D., Blair, J. M., Bridgham, S. D., Burton, A. J.,
910 Carrillo, Y., Reich, P. B., Clark, J. S., Classen, A. T., Dijkstra, F. A., Elberling, B., Emmett, B. A.,
911 Estiarte, M., Frey, S. D., Guo, J., Harte, J., Jiang, L., Johnson, B. R., Kröel-Dulay, G., Larsen, K. S.,
912 Laudon, H., Lavallee, J. M., Luo, Y., Lupascu, M., Ma, L. N., Marhan, S., Michelsen, A., Mohan, J.,
913 Niu, S., Pendall, E., Peñuelas, J., Pfeifer-Meister, L., Poll, C., Reinsch, S., Reynolds, L. L., Schmidt,
914 I. K., Sistla, S., Sokol, N. W., Templer, P. H., Treseder, K. K., Welker, J. M. and Bradford, M. A.:
915 Quantifying global soil carbon losses in response to warming, Nature, 540(7631), 104–108,
916 doi:10.1038/nature20150, 2016.

917 Cuny, H. E., Rathgeber, C. B. K., Lebourgeois, F., Fortin, M. and Fournier, M.: Life strategies in
918 intra-annual dynamics of wood formation: example of three conifer species in a temperate
919 forest in north-east France, Tree Physiology, 32(5), 612–625, doi:10.1093/treephys/tps039,
920 2012.

921 Curtis, P. S., Hanson, P. J., Bolstad, P., Barford, C., Randolph, J. C., Schmid, H. P. and Wilson, K.
922 B.: Biometric and eddy-covariance based estimates of annual carbon storage in five eastern
923 North American deciduous forests, Agricultural and Forest Meteorology, 113(1–4), 3–19,
924 doi:10.1016/S0168-1923(02)00099-0, 2002.

925 Davidson, E. A. and Janssens, I. A.: Temperature sensitivity of soil carbon decomposition and
926 feedbacks to climate change, Nature, 440(7081), 165–173, doi:10.1038/nature04514, 2006.

927 De Kauwe, M. G., Medlyn, B. E., Zaehle, S., Walker, A. P., Dietze, M. C., Wang, Y.-P., Luo, Y., Jain,
928 A. K., El-Masri, B., Hickler, T., Wårlind, D., Weng, E., Parton, W. J., Thornton, P. E., Wang, S.,
929 Prentice, I. C., Asao, S., Smith, B., McCarthy, H. R., Iversen, C. M., Hanson, P. J., Warren, J. M.,
930 Oren, R. and Norby, R. J.: Where does the carbon go? A model-data intercomparison of
931 vegetation carbon allocation and turnover processes at two temperate forest free-air CO_2
932 enrichment sites, New Phytologist, 203(3), 883–899, doi:10.1111/nph.12847, 2014.

933 Deak, K. I. and Malamy, J.: Osmotic regulation of root system architecture, The Plant Journal,
934 43(1), 17–28, doi:10.1111/j.1365-313X.2005.02425.x, 2005.

935 DeAngelis, D. L., Ju, S., Liu, R., Bryant, J. P. and Gourley, S. A.: Plant allocation of carbon to
936 defense as a function of herbivory, light and nutrient availability, Theoretical Ecology, 5(3), 445–
937 456, doi:10.1007/s12080-011-0135-z, 2012.

938 Douma, J. C., de Haan, M. W. A., Aerts, R., Witte, J.-P. M. and van Bodegom, P. M.: Succession-
939 induced trait shifts across a wide range of NW European ecosystems are driven by light and
940 modulated by initial abiotic conditions: Trait shifts during succession, Journal of Ecology, 100(2),
941 366–380, doi:10.1111/j.1365-2745.2011.01932.x, 2012.

942 Drake, J. E., Gallet-Budynek, A., Hofmockel, K. S., Bernhardt, E. S., Billings, S. A., Jackson, R. B.,
943 Johnsen, K. S., Lichter, J., McCarthy, H. R., McCormack, M. L., Moore, D. J. P., Oren, R.,
944 Palmroth, S., Phillips, R. P., Pippen, J. S., Pritchard, S. G., Treseder, K. K., Schlesinger, W. H.,

DeLucia, E. H. and Finzi, A. C.: Increases in the flux of carbon belowground stimulate nitrogen uptake and sustain the long-term enhancement of forest productivity under elevated CO2, ECOLOGY LETTERS, 14(4), 349–357, doi:10.1111/j.1461-0248.2011.01593.x, 2011.

Dudley, S. A. and Schmitt, J.: Testing the adaptive plasticity hypothesis: density-dependent selection on manipulated stem length in Impatiens capensis, The American Naturalist, 147(3), 445–465, doi:10.1086/285860, 1996.

Dybzinski, R., Farrior, C., Wolf, A., Reich, P. B. and Pacala, S. W.: Evolutionarily Stable Strategy Carbon Allocation to Foliage, Wood, and Fine Roots in Trees Competing for Light and Nitrogen: An Analytically Tractable, Individual-Based Model and Quantitative Comparisons to Data, American Naturalist, 177(2), 153–166, doi:10.1086/657992, 2011.

Dybzinski, R., Farrior, C. E. and Pacala, S. W.: Increased forest carbon storage with increased atmospheric CO2 despite nitrogen limitation: a game-theoretic allocation model for trees in competition for nitrogen and light, Global Change Biology, 21(3), 1182–1196, doi:10.1111/gcb.12783, 2015.

Dybzinski, R., Kelvakis, A., McCabe, J., Panock, S., Anuchitlertchon, K., Vasarhelyi, L., Luke McCormack, M., McNickle, G. G., Poorter, H., Trinder, C. and Farrior, C. E.: How are nitrogen availability, fine-root mass, and nitrogen uptake related empirically? Implications for models and theory, Global Change Biology, doi:10.1111/gcb.14541, 2019.

Emanuel, W. R. and Killough, G. G.: Modeling terrestrial ecosystems in the global carbon cycle with Shifts in carbon storage capacity by land-use change, Ecology, 65(3), 970–983, doi:10.2307/1938069, 1984.

Eriksson, E.: Compartment Models and Reservoir Theory, Annual Review of Ecology and Systematics, 2(1), 67–84, doi:10.1146/annurev.es.02.110171.000435, 1971.

Falster, D. and Westoby, M.: Plant height and evolutionary games, TRENDS IN ECOLOGY & EVOLUTION, 18(7), 337–343, doi:10.1016/S0169-5347(03)00061-2, 2003.

Farrior, C. E., Dybzinski, R., Levin, S. A. and Pacala, S. W.: Competition for Water and Light in Closed-Canopy Forests: A Tractable Model of Carbon Allocation with Implications for Carbon Sinks, American Naturalist, 181(3), 314–330, doi:10.1086/669153, 2013.

Farrior, C. E., Rodriguez-Iturbe, I., Dybzinski, R., Levin, S. A. and Pacala, S. W.: Decreased water limitation under elevated CO2 amplifies potential for forest carbon sinks, Proceedings of the National Academy of Sciences of the United States of America, 112(23), 7213–7218, doi:10.1073/pnas.1506262112, 2015.

Fatichi, S., Pappas, C., Zscheischler, J. and Leuzinger, S.: Modelling carbon sources and sinks in terrestrial vegetation, New Phytologist, 221(2), 652–668, doi:10.1111/nph.15451, 2019.

Fisher, R. A., Koven, C. D., Anderegg, W. R. L., Christoffersen, B. O., Dietze, M. C., Farrior, C. E., Holm, J. A., Hurtt, G. C., Knox, R. G., Lawrence, P. J., Lichstein, J. W., Longo, M., Matheny, A. M., Medvigy, D., Muller-Landau, H. C., Powell, T. L., Serbin, S. P., Sato, H., Shuman, J. K., Smith, B., Trugman, A. T., Viskari, T., Verbeeck, H., Weng, E., Xu, C., Xu, X., Zhang, T. and Moorcroft, P. R.: Vegetation demographics in Earth System Models: A review of progress and priorities, Global Change Biology, 24(1), 35–54, doi:10.1111/gcb.13910, 2018.

Franklin, O., Johansson, J., Dewar, R. C., Dieckmann, U., McMurtrie, R. E., Brannstrom, A. and Dybzinski, R.: Modeling carbon allocation in trees: a search for principles, Tree Physiology, 32(6), 648–666, doi:10.1093/treephys/tpr138, 2012.

Friend, A. D., Arneth, A., Kiang, N. Y., Lomas, M., Ogee, J., Roedenbeckk, C., Running, S. W., Santaren, J.-D., Sitch, S., Viovy, N., Woodward, F. I. and Zaehle, S.: FLUXNET and modelling the global carbon cycle, Global Change Biology, 13(3), 610–633, doi:10.1111/j.1365-2486.2006.01223.x, 2007.

Gersani, M., Brown, J. s., O'Brien, E. E., Maina, G. M. and Abramsky, Z.: Tragedy of the commons as a result of root competition, Journal of Ecology, 89(4), 660–669, doi:10.1046/j.0022-0477.2001.00609.x, 2001.

Givnish, T.: Adaptive significance of evergreen vs. deciduous leaves: solving the triple paradox, Silva Fenn., 36(3), doi:10.14214/sf.535, 2002.

Givnish, T. J.: On the Adaptive Significance of Leaf Height in Forest Herbs, The American Naturalist, 120(3), 353–381, doi:10.1086/283995, 1982.

Goldschmidt, E. E. and Huber, S. C.: Regulation of Photosynthesis by End-Product Accumulation in Leaves of Plants Storing Starch, Sucrose, and Hexose Sugars, Plant Physiology, 99(4), 1443–1448, doi:10.1104/pp.99.4.1443, 1992.

Gower, S. T., Krankina, O., Olson, R. J., Apps, M., Linder, S. and Wang, C.: Net Primary Production and Carbon Allocation Patterns of Boreal Forest Ecosystems, Ecological Applications, 11(5), 1395–1411, doi:10.1890/1051-0761(2001)011[1395:NPPACA]2.0.CO;2, 2001.

Grams, T. E. E. and Andersen, C. P.: Competition for Resources in Trees: Physiological Versus Morphological Plasticity, in Progress in Botany, edited by K. Esser, U. Löttge, W. Beyschlag, and J. Murata, pp. 356–381, Springer Berlin Heidelberg, Berlin, Heidelberg., 2007.

Haverd, V., Smith, B., Raupach, M., Briggs, P., Nieradzik, L., Beringer, J., Hutley, L., Trudinger, C. M. and Cleverly, J.: Coupling carbon allocation with leaf and root phenology predicts tree–grass partitioning along a savanna rainfall gradient, Biogeosciences, 13(3), 761–779, doi:10.5194/bg-13-761-2016, 2016.

Hibbs, D. E.: Forty Years of Forest Succession in Central New England, Ecology, 64(6), 1394–1401, doi:10.2307/1937493, 1983.

Hodge, A.: Root decisions, Plant, Cell & Environment, 32(6), 628–640, doi:10.1111/j.1365-3040.2008.01891.x, 2009.

Hoffman, F. M., Koven, C. D., Keppel-Aleks, G., Lawrence, D. M., Riley, W. J., Randerson, J. T., Ahlström, A., Abramowitz, G., Baldocchi, D. D., Best, M. J., Bond-Lamberty, B., De Kauwe, M. G., Denning, A. S., Desai, A. R., Eyring, V., Fisher, J. B., Fisher, R. A., Gleckler, P. J., Huang, M., Hugelius, G., Jain, A. K., Kiang, N. Y., Kim, H., Koster, R. D., Kumar, S. V., Li, H., Luo, Y., Mao, J., McDowell, N. G., Mishra, U., Moorcroft, P. R., Pau, G. S. H., Ricciuto, D. M., Schaefer, K., Schwalm, C. R., Serbin, S. P., Shevliakova, E., Slater, A. G., Tang, J., Williams, M., Xia, J., Xu, C., Joseph, R. and Koch, D.: 2016 International Land Model Benchmarking (ILAMB) Workshop Report., 2017.

Iversen, C. M.: Digging deeper: fine-root responses to rising atmospheric CO2 concentration in forested ecosystems, New Phytologist, 186(2), 346–357, doi:10.1111/j.1469-8137.2009.03122.x, 2010.

Jackson, R. B., Cook, C. W., Pippen, J. S. and Palmer, S. M.: Increased belowground biomass and soil CO2 fluxes after a decade of carbon dioxide enrichment in a warm-temperate forest, Ecology, 90(12), 3352–3366, doi:10.1890/08-1609.1, 2009.

Jenkins, J. C., Chojnacky, D. C., Heath, L. S. and Birdsey, R. A.: National-Scale Biomass Estimators for United States Tree Species, Forest Science, 49(1), 12–35, doi:10.1093/forestscience/49.1.12, 2003.

Jiang, M., Medlyn, B. E., Drake, J. E., Duursma, R. A., Anderson, I. C., Barton, C. V. M., Boer, M. M., Carrillo, Y., Castañeda-Gómez, L., Collins, L., Crous, K. Y., De Kauwe, M. G., Emmerson, K. M., Facey, S. L., Gherlenda, A. N., Gimeno, T. E., Hasegawa, S., Johnson, S. N., Macdonald, C. A., Mahmud, K., Moore, B. D., Nazaries, L., Nielsen, U. N., Noh, N. J., Ochoa-Hueso, R., Pathare, V. S., Pendall, E., Pineiro, J., Powell, J. R., Power, S. A., Reich, P. B., Renchon, A. A., Riegler, M., Rymer, P., Salomón, R. L., Singh, B. K., Smith, B., Tjoelker, M. G., Walker, J. K. M., Wujeska-Klause, A., Yang, J., Zaehle, S. and Ellsworth, D. S.: The fate of carbon in a mature forest under carbon dioxide enrichment, preprint, Ecology., 2019a.

Jiang, M., Zaehle, S., De Kauwe, M. G., Walker, A. P., Caldararu, S., Ellsworth, D. S. and Medlyn, B. E.: The quasi-equilibrium framework revisited: analyzing long-term CO2 enrichment responses in plant–soil models, Geosci. Model Dev., 12(5), 2069–2089, doi:10.5194/gmd-12-2069-2019, 2019b.

Keenan, T. F., Davidson, E. A., Munger, J. W. and Richardson, A. D.: Rate my data: quantifying the value of ecological data for the development of models of the terrestrial carbon cycle, Ecological Applications, 23(1), 273–286, doi:10.1890/12-0747.1, 2013.

Körner, C.: Plant CO2 responses: an issue of definition, time and resource supply, New Phytol, 172(3), 393–411, doi:10.1111/j.1469-8137.2006.01886.x, 2006.

Koven, C. D., Chambers, J. Q., Georgiou, K., Knox, R., Negron-Juarez, R., Riley, W. J., Arora, V. K., Brovkin, V., Friedlingstein, P. and Jones, C. D.: Controls on terrestrial carbon feedbacks by productivity versus turnover in the CMIP5 Earth System Models, Biogeosciences, 12(17), 5211–5228, doi:10.5194/bg-12-5211-2015, 2015.

Krinner, G., Viovy, N., de Noblet-Ducoudré, N., Ogée, J., Polcher, J., Friedlingstein, P., Ciais, P., Sitch, S. and Prentice, I. C.: A dynamic global vegetation model for studies of the coupled atmosphere-biosphere system, Global Biogeochemical Cycles, 19(1), doi:10.1029/2003GB002199, 2005.

Kulmatiski, A., Adler, P. B., Stark, J. M. and Tredennick, A. T.: Water and nitrogen uptake are better associated with resource availability than root biomass, Ecosphere, 8(3), e01738, doi:10.1002/ecs2.1738, 2017.

Lacointe, A.: Carbon allocation among tree organs: A review of basic processes and representation in functional-structural tree models, Annals of Forest Science, 57(5), 521–533, doi:10.1051/forest:2000139, 2000.

Leuning, R., Kelliher, F. M., Pury, D. G. G. and Schulze, E.-D.: Leaf nitrogen, photosynthesis, conductance and transpiration: scaling from leaves to canopies, Plant Cell Environ, 18(10), 1183–1200, doi:10.1111/j.1365-3040.1995.tb00628.x, 1995.

Linkohr, B. I., Williamson, L. C., Fitter, A. H. and Leyser, H. M. O.: Nitrate and phosphate availability and distribution have different effects on root system architecture of Arabidopsis, The Plant Journal, 29(6), 751–760, doi:10.1046/j.1365-313X.2002.01251.x, 2002.

Litton, C., Ryan, M., Knight, D. and Stahl, P.: Soil-surface carbon dioxide efflux and microbial biomass in relation to tree density 13 years after a stand replacing fire in a lodgepole pine ecosystem, GLOBAL CHANGE BIOLOGY, 9(5), 680–696, doi:10.1046/j.1365-2486.2003.00626.x, 2003.

Litton, C. M., Raich, J. W. and Ryan, M. G.: Carbon allocation in forest ecosystems, Global Change Biol, 13(10), 2089–2109, doi:10.1111/j.1365-2486.2007.01420.x, 2007.

Luo, Y. and Weng, E.: Dynamic disequilibrium of the terrestrial carbon cycle under global change, Trends in Ecology & Evolution, 26(2), 96–104, doi:10.1016/j.tree.2010.11.003, 2011.

Luo, Y., Hui, D. and Zhang, D.: Elevated CO2 stimulates net accumulations of carbon and nitrogen in land ecosystems: a meta-analysis, Ecology, 87(1), 53–63, 2006.

Luo, Y. Q., Wu, L. H., Andrews, J. A., White, L., Matamala, R., Schafer, K. V. R. and Schlesinger, W. H.: Elevated CO2 differentiates ecosystem carbon processes: Deconvolution analysis of Duke Forest FACE data, Ecological Monographs, 71(3), 357–376, doi:10.1890/0012-9615(2001)071[0357:ECDECP]2.0.CO;2, 2001.

1084 Luo, Y. Q., Randerson, J. T., Abramowitz, G., Bacour, C., Blyth, E., Carvalhais, N., Ciais, P.,
1085 Dalmonech, D., Fisher, J. B., Fisher, R., Friedlingstein, P., Hibbard, K., Hoffman, F., Huntzinger,
1086 D., Jones, C. D., Koven, C., Lawrence, D., Li, D. J., Mahecha, M., Niu, S. L., Norby, R., Piao, S. L.,
1087 Qi, X., Peylin, P., Prentice, I. C., Riley, W., Reichstein, M., Schwalm, C., Wang, Y. P., Xia, J. Y.,
1088 Zaehle, S. and Zhou, X. H.: A framework for benchmarking land models, Biogeosciences, 9(10),
1089 3857–3874, doi:10.5194/bg-9-3857-2012, 2012.

1090 Magill, A. H., Aber, J. D., Currie, W. S., Nadelhoffer, K. J., Martin, M. E., McDowell, W. H., Melillo,
1091 J. M. and Steudler, P.: Ecosystem response to 15 years of chronic nitrogen additions at the
1092 Harvard Forest LTER, Massachusetts, USA, Forest Ecology and Management, 196(1), 7–28,
1093 doi:10.1016/j.foreco.2004.03.033, 2004.

1094 Mäkelä, A., Valentine, H. T. and Helmisaari, H.-S.: Optimal co-allocation of carbon and nitrogen
1095 in a forest stand at steady state, New Phytologist, 180(1), 114–123, doi:10.1111/j.1469-
1096 8137.2008.02558.x, 2008.

1097 Martin, A. R., Gezahegn, S. and Thomas, S. C.: Variation in carbon and nitrogen concentration
1098 among major woody tissue types in temperate trees, Can. J. For. Res., 45(6), 744–757,
1099 doi:10.1139/cjfr-2015-0024, 2015.

1100 McDowell, N., Barnard, H., Bond, B., Hinckley, T., Hubbard, R., Ishii, H., Köstner, B., Magnani, F.,
1101 Marshall, J., Meinzer, F., Phillips, N., Ryan, M. and Whitehead, D.: The relationship between
1102 tree height and leaf area: sapwood area ratio, Oecologia, 132(1), 12–20, doi:10.1007/s00442-
1103 002-0904-x, 2002.

1104 McGill, B. J. and Brown, J. S.: Evolutionary Game Theory and Adaptive Dynamics of Continuous
1105 Traits, Annual Review of Ecology, Evolution, and Systematics, 38(1), 403–435,
1106 doi:10.1146/annurev.ecolsys.36.091704.175517, 2007.

1107 McMurtrie, R. E., Iversen, C. M., Dewar, R. C., Medlyn, B. E., Näsholm, T., Pepper, D. A. and
1108 Norby, R. J.: Plant root distributions and nitrogen uptake predicted by a hypothesis of optimal
1109 root foraging, Ecology and Evolution, 2(6), 1235–1250, doi:10.1002/ece3.266, 2012.

1110 McNickle, G. G. and Brown, J. S.: An ideal free distribution explains the root production of
1111 plants that do not engage in a tragedy of the commons game, edited by S. Schwinning, Journal
1112 of Ecology, 102(4), 963–971, doi:10.1111/1365-2745.12259, 2014.

1113 McNickle, G. G. and Dybzinski, R.: Game theory and plant ecology, edited by J. Klironomos,
1114 Ecology Letters, 16(4), 545–555, doi:10.1111/ele.12071, 2013.

1115 Melillo, J. M., Butler, S., Johnson, J., Mohan, J., Steudler, P., Lux, H., Burrows, E., Bowles, F.,
1116 Smith, R., Scott, L., Vario, C., Hill, T., Burton, A., Zhou, Y.-M. and Tang, J.: Soil warming, carbon-
1117 nitrogen interactions, and forest carbon budgets, Proceedings of the National Academy of
1118 Sciences, 108(23), 9508–9512, doi:10.1073/pnas.1018189108, 2011.

Menge, D. N. L., Batterman, S. A., Hedin, L. O., Liao, W., Pacala, S. W. and Taylor, B. N.: Why are nitrogen-fixing trees rare at higher compared to lower latitudes?, Ecology, 98(12), 3127–3140, doi:10.1002/ecy.2034, 2017.

Michelot, A., Simard, S., Rathgeber, C., Dufrene, E. and Damesin, C.: Comparing the intra-annual wood formation of three European species (Fagus sylvatica, Quercus petraea and Pinus sylvestris) as related to leaf phenology and non-structural carbohydrate dynamics, Tree Physiology, 32(8), 1033–1045, doi:10.1093/treephys/tps052, 2012.

Montané, F., Fox, A. M., Arellano, A. F., MacBean, N., Alexander, M. R., Dye, A., Bishop, D. A., Trouet, V., Babst, F., Hessl, A. E., Pederson, N., Blanken, P. D., Bohrer, G., Gough, C. M., Litvak, M. E., Novick, K. A., Phillips, R. P., Wood, J. D. and Moore, D. J. P.: Evaluating the effect of alternative carbon allocation schemes in a land surface model (CLM4.5) on carbon fluxes, pools, and turnover in temperate forests, Geoscientific Model Development, 10(9), 3499–3517, doi:10.5194/gmd-10-3499-2017, 2017.

Moorcroft, P. R., Hurtt, G. C. and Pacala, S. W.: A method for scaling vegetation dynamics: The ecosystem demography model (ED), Ecological Monographs, 71(4), 557–585, doi:10.1890/0012-9615(2001)071[0557:AMFSVD]2.0.CO;2, 2001.

Morris, E. C., Griffiths, M., Golebiowska, A., Mairhofer, S., Burr-Hersey, J., Goh, T., Wangenheim, D. von, Atkinson, B., Sturrock, C. J., Lynch, J. P., Vissenberg, K., Ritz, K., Wells, D. M., Mooney, S. J. and Bennett, M. J.: Shaping 3D Root System Architecture, Current Biology, 27(17), R919–R930, doi:10.1016/j.cub.2017.06.043, 2017.

Nie, M., Lu, M., Bell, J., Raut, S. and Pendall, E.: Altered root traits due to elevated CO2: a meta-analysis: Root traits at elevated CO2, Global Ecology and Biogeography, 22(10), 1095–1105, doi:10.1111/geb.12062, 2013.

Norby, R. J. and Zak, D. R.: Ecological Lessons from Free-Air CO2 Enrichment (FACE) Experiments, Annual Review of Ecology, Evolution, and Systematics, 42(1), 181–203, doi:10.1146/annurev-ecolsys-102209-144647, 2011.

Norby, R. J., Sholtis, J. D., Gunderson, C. A. and Jawdy, S. S.: Leaf dynamics of a deciduous forest canopy: no response to elevated CO 2, Oecologia, 136(4), 574–584, doi:10.1007/s00442-003-1296-2, 2003.

O'Brien, E. E., Gersani, M. and Brown, J. S.: Root proliferation and seed yield in response to spatial heterogeneity of below-ground competition, New Phytologist, 168(2), 401–412, doi:10.1111/j.1469-8137.2005.01520.x, 2005.

Ordoñez, J. C., van Bodegom, P. M., Witte, J.-P. M., Wright, I. J., Reich, P. B. and Aerts, R.: A global study of relationships between leaf traits, climate and soil measures of nutrient fertility, Global Ecology and Biogeography, 18(2), 137–149, doi:10.1111/j.1466-8238.2008.00441.x, 2009.

Oyewole, O. A., Inselsbacher, E., Näsholm, T. and Jämtgård, S.: Incorporating mass flow strongly promotes N flux rates in boreal forest soils, Soil Biology and Biochemistry, 114, 263–269, doi:10.1016/j.soilbio.2017.07.021, 2017.

Pappas, C., Fatichi, S. and Burlando, P.: Modeling terrestrial carbon and water dynamics across climatic gradients: does plant trait diversity matter?, New Phytologist, 209(1), 137–151, doi:10.1111/nph.13590, 2016.

Parton, W., Schimel, D., Cole, C. and Ojima, D.: Analysis of factors controlling soil organic matter levels in Great Plains grasslands, Soil Science Society of America Journal, 51(5), 1173–1179, doi:10.2136/sssaj1987.03615995005100050015x, 1987.

Phillips, R. P., Finzi, A. C. and Bernhardt, E. S.: Enhanced root exudation induces microbial feedbacks to N cycling in a pine forest under long-term CO2 fumigation, Ecology Letters, 14(2), 187–194, doi:10.1111/j.1461-0248.2010.01570.x, 2011.

Phillips, R. P., Brzostek, E. and Midgley, M. G.: The mycorrhizal-associated nutrient economy: a new framework for predicting carbon-nutrient couplings in temperate forests, New Phytologist, 199(1), 41–51, doi:10.1111/nph.12221, 2013.

Plomion, C., Leprovost, G. and Stokes, A.: Wood Formation in Trees, PLANT PHYSIOLOGY, 127(4), 1513–1523, doi:10.1104/pp.010816, 2001.

Poorter, H., Niklas, K. J., Reich, P. B., Oleksyn, J., Poot, P. and Mommer, L.: Biomass allocation to leaves, stems and roots: meta-analyses of interspecific variation and environmental control: Tansley review, New Phytologist, 193(1), 30–50, doi:10.1111/j.1469-8137.2011.03952.x, 2012.

Post, W. M., Pastor, J., Zinke, P. J. and Stangenberger, A. G.: Global patterns of soil nitrogen storage, Nature, 317(6038), 613–616, doi:10.1038/317613a0, 1985.

Pregitzer, K. S., Hendrick, R. L. and Fogel, R.: The demography of fine roots in response to patches of water and nitrogen, New Phytologist, 125(3), 575–580, doi:10.1111/j.1469-8137.1993.tb03905.x, 1993.

Pregitzer, K. S., DeForest, J. L., Burton, A. J., Allen, M. F., Ruess, R. W. and Hendrick, R. L.: Fine Root Architecture of Nine North American Trees, Ecological Monographs, 72(2), 293, doi:10.2307/3100029, 2002.

Raich, J., Rastetter, E. B., Melillo, J. M., Kicklighter, D. W., Steudler, P. A., Peterson, B. J., Grace, A., Moore, B. and Vorosmary, C. J.: Potential Net Primary Productivity in South America: Application of a Global Model, Ecological Applications, 1(4), 399–429, doi:10.2307/1941899, 1991.

Randerson, J., Thompson, M., Conway, T., Fung, I. and Field, C.: The contribution of terrestrial sources and sinks to trends in the seasonal cycle of atmospheric carbon dioxide, Global Biogeochemical Cycles, 11(4), 535–560, doi:10.1029/97GB02268, 1997.

Reich, P. B., Luo, Y., Bradford, J. B., Poorter, H., Perry, C. H. and Oleksyn, J.: Temperature drives global patterns in forest biomass distribution in leaves, stems, and roots, Proceedings of the National Academy of Sciences, 111(38), 13721–13726, doi:10.1073/pnas.1216053111, 2014.

Savage, K. E., Parton, W. J., Davidson, E. A., Trumbore, S. E. and Frey, S. D.: Long-term changes in forest carbon under temperature and nitrogen amendments in a temperate northern hardwood forest, Global Change Biology, 19(8), 2389–2400, doi:10.1111/gcb.12224, 2013.

Scheiter, S. and Higgins, S. I.: Impacts of climate change on the vegetation of Africa: an adaptive dynamic vegetation modelling approach, Global Change Biology, 15(9), 2224–2246, doi:10.1111/j.1365-2486.2008.01838.x, 2009.

Scheiter, S., Langan, L. and Higgins, S. I.: Next-generation dynamic global vegetation models: learning from community ecology, New Phytologist, 198(3), 957–969, doi:10.1111/nph.12210, 2013.

Schmidt, G. A., Kelley, M., Nazarenko, L., Ruedy, R., Russell, G. L., Aleinov, I., Bauer, M., Bauer, S. E., Bhat, M. K., Bleck, R., Canuto, V., Chen, Y.-H., Cheng, Y., Clune, T. L., Del Genio, A., de Fainchtein, R., Faluvegi, G., Hansen, J. E., Healy, R. J., Kiang, N. Y., Koch, D., Lacis, A. A., LeGrande, A. N., Lerner, J., Lo, K. K., Matthews, E. E., Menon, S., Miller, R. L., Oinas, V., Oloso, A. O., Perlwitz, J. P., Puma, M. J., Putman, W. M., Rind, D., Romanou, A., Sato, M., Shindell, D. T., Sun, S., Syed, R. A., Tausnev, N., Tsigaridis, K., Unger, N., Voulgarakis, A., Yao, M.-S. and Zhang, J.: Configuration and assessment of the GISS ModelE2 contributions to the CMIP5 archive, Journal of Advances in Modeling Earth Systems, 6(1), 141–184, doi:10.1002/2013MS000265, 2014.

Shevliakova, E., Pacala, S. W., Malyshev, S., Hurtt, G. C., Milly, P. C. D., Caspersen, J. P., Sentman, L. T., Fisk, J. P., Wirth, C. and Crevoisier, C.: Carbon cycling under 300 years of land use change: Importance of the secondary vegetation sink, Global Biogeochemical Cycles, 23, GB2022, doi:10.1029/2007GB003176, 2009.

Shinozaki, Kichiro, Yoda, Kyoji, Hozumi, Kazuo and Kira, Tatuo: A quantitative analysis of plant form – the pipe model theory. I. Basic analyses, Japanese Journal of Ecology, 14(3), 97–105, 1964.

Sierra, C. A. and Mueller, M.: A general mathematical framework for representing soil organic matter dynamics, Ecological Monographs, 85(4), 505–524, doi:10.1890/15-0361.1, 2015.

Sierra, C. A., Muller, M., Metzler, H., Manzoni, S. and Trumbore, S. E.: The muddle of ages, turnover, transit, and residence times in the carbon cycle, Global Change Biology, 23(5), 1763–1773, doi:10.1111/gcb.13556, 2017.

Sitch, S., Smith, B., Prentice, I. C., Arneth, A., Bondeau, A., Cramer, W., Kaplan, J. O., Levis, S., Lucht, W., Sykes, M. T., Thonicke, K. and Venevsky, S.: Evaluation of ecosystem dynamics, plant

geography and terrestrial carbon cycling in the LPJ dynamic global vegetation model, Global Change Biology, 9(2), 161–185, doi:10.1046/j.1365-2486.2003.00569.x, 2003.

Smith, A. R., Lukac, M., Bambrick, M., Miglietta, F. and Godbold, D. L.: Tree species diversity interacts with elevated CO2 to induce a greater root system response, Glob Change Biol, 19(1), 217–228, doi:10.1111/gcb.12039, 2013.

Soriano, D., Orozco-Segovia, A., Márquez-Guzmán, J., Kitajima, K., Gamboa-de Buen, A. and Huante, P.: Seed reserve composition in 19 tree species of a tropical deciduous forest in Mexico and its relationship to seed germination and seedling growth, Annals of Botany, 107(6), 939–951, doi:10.1093/aob/mcr041, 2011.

Strigul, N., Pristinski, D., Purves, D., Dushoff, J. and Pacala, S.: Scaling from trees to forests: tractable macroscopic equations for forest dynamics, Ecological Monographs, 78(4), 523–545, doi:10.1890/08-0082.1, 2008.

Sulman, B. N., Phillips, R. P., Oishi, A. C., Shevliakova, E. and Pacala, S. W.: Microbe-driven turnover offsets mineral-mediated storage of soil carbon under elevated CO2, Nature Climate Change, 4(12), 1099–1102, doi:10.1038/NCLIMATE2436, 2014.

Tilman, D.: Plant strategies and the dynamics and structure of plant communities, Princeton University Press, Princeton, N.J., 1988.

Urbanski, S., Barford, C., Wofsy, S., Kucharik, C., Pyle, E., Budney, J., McKain, K., Fitzjarrald, D., Czikowsky, M. and Munger, J. W.: Factors controlling CO2 exchange on timescales from hourly to decadal at Harvard Forest, Journal of Geophysical Research - Biogeosciences, 112(G2), doi:10.1029/2006JG000293, 2007.

Valentine, H. T. and Mäkelä, A.: Modeling forest stand dynamics from optimal balances of carbon and nitrogen, New Phytologist, 194(4), 961–971, doi:10.1111/j.1469-8137.2012.04123.x, 2012.

Vitousek, P. M., Menge, D. N. L., Reed, S. C. and Cleveland, C. C.: Biological nitrogen fixation: rates, patterns and ecological controls in terrestrial ecosystems, Philosophical Transactions of the Royal Society B: Biological Sciences, 368(1621), 20130119–20130119, doi:10.1098/rstb.2013.0119, 2013.

Walker, A. P., De Kauwe, M. G., Medlyn, B. E., Zaehle, S., Iversen, C. M., Asao, S., Guenet, B., Harper, A., Hickler, T., Hungate, B. A., Jain, A. K., Luo, Y., Lu, X., Lu, M., Luus, K., Megonigal, J. P., Oren, R., Ryan, E., Shu, S., Talhelm, A., Wang, Y.-P., Warren, J. M., Werner, C., Xia, J., Yang, B., Zak, D. R. and Norby, R. J.: Decadal biomass increment in early secondary succession woody ecosystems is increased by CO2 enrichment, Nat Commun, 10(1), 454, doi:10.1038/s41467-019-08348-1, 2019.

Weng, E., Farrior, C. E., Dybzinski, R. and Pacala, S. W.: Predicting vegetation type through physiological and environmental interactions with leaf traits: evergreen and deciduous forests

in an earth system modeling framework, Global Change Biology, 23(6), 2482–2498, doi:10.1111/gcb.13542, 2017.

Weng, E. S., Malyshev, S., Lichstein, J. W., Farrior, C. E., Dybzinski, R., Zhang, T., Shevliakova, E. and Pacala, S. W.: Scaling from individual trees to forests in an Earth system modeling framework using a mathematically tractable model of height-structured competition, Biogeosciences, 12(9), 2655–2694, doi:10.5194/bg-12-2655-2015, 2015.

Wieder, W. R., Grandy, A. S., Kallenbach, C. M. and Bonan, G. B.: Integrating microbial physiology and physio-chemical principles in soils with the MIcrobial-MIneral Carbon Stabilization (MIMICS) model, BIOGEOSCIENCES, 11(14), 3899–3917, doi:10.5194/bg-11-3899-2014, 2014.

Wieder, W. R., Allison, S. D., Davidson, E. A., Georgiou, K., Hararuk, O., He, Y., Hopkins, F., Luo, Y., Smith, M. J., Sulman, B., Todd-Brown, K., Wang, Y.-P., Xia, J. and Xu, X.: Explicitly representing soil microbial processes in Earth system models, GLOBAL BIOGEOCHEMICAL CYCLES, 29(10), 1782–1800, doi:10.1002/2015GB005188, 2015.

Wright, I., Reich, P., Westoby, M., Ackerly, D., Baruch, Z., Bongers, F., Cavender-Bares, J., Chapin, T., Cornelissen, J., Diemer, M., Flexas, J., Garnier, E., Groom, P., Gulias, J., Hikosaka, K., Lamont, B., Lee, T., Lee, W., Lusk, C., Midgley, J., Navas, M., Niinemets, U., Oleksyn, J., Osada, N., Poorter, H., Poot, P., Prior, L., Pyankov, V., Roumet, C., Thomas, S., Tjoelker, M., Veneklaas, E. and Villar, R.: The worldwide leaf economics spectrum, NATURE, 428(6985), 821–827, doi:10.1038/nature02403, 2004.

Xia, J., Luo, Y., Wang, Y.-P. and Hararuk, O.: Traceable components of terrestrial carbon storage capacity in biogeochemical models, Global Change Biology, 19(7), 2104–2116, doi:10.1111/gcb.12172, 2013.

Yang, Y., Luo, Y. and Finzi, A. C.: Carbon and nitrogen dynamics during forest stand development: a global synthesis, New Phytologist, 190(4), 977–989, doi:10.1111/j.1469-8137.2011.03645.x, 2011.

Zadworny, M., McCormack, M. L., Mucha, J., Reich, P. B. and Oleksyn, J.: Scots pine fine roots adjust along a 2000-km latitudinal climatic gradient, New Phytologist, 212(2), 389–399, doi:10.1111/nph.14048, 2016.

Zea-Cabrera, E., Iwasa, Y., Levin, S. and Rodríguez-Iturbe, I.: Tragedy of the commons in plant water use, Water Resources Research, 42(6), W06D02, doi:10.1029/2005WR004514, 2006.